AD-A086 831 FLOW RESEARCH CO KENT WA F/G 20/4
VISUALIZATION STUDY OF TURBULENT SPOTS.(U)
MAY 80 M GAD-EL-HAK, J J RILEY F49620-78-C-0062
UNCLASSIFIED FLOW-RR-162 AFOSR-TR-80-0473 NL

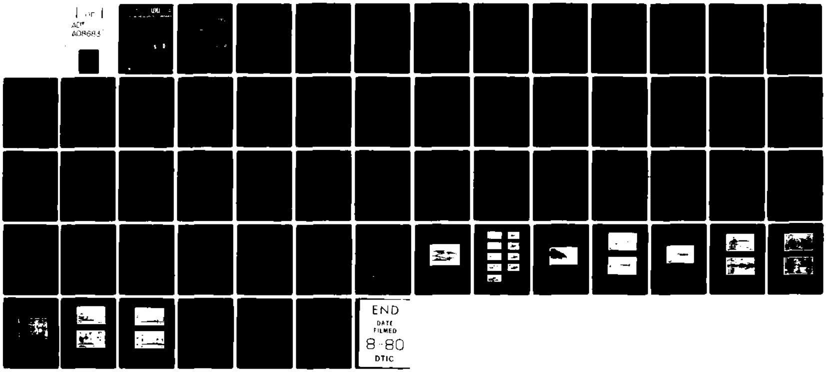

AFOSR-TR- 80-0473

LEVEL II

(12)

FLOW RESEARCH COMPANY

A DIVISION OF FLOW INDUSTRIES, INC.

Approved for public release;
distribution unlimited.

HEADQUARTERS
21414 - 68th Avenue South
Kent, Washington 98031 (206) 854-1370
Seattle Ex. 622-1500 TWX 910-447-2762

12

LEVEL II

Flow Research Report No. 162

Visualization Study of Turbulent Spots*

Interim ([redacted] Technical Report)

By

Mohamed Gad-el-Hak
And
James J. Riley

May 1980

Flow Research Company
A Division of Flow Industries, Inc.
21414-68th Avenue South
Kent, Washington 98031
(206) 854-1370

*Research Sponsored by the Air Force Office of Scientific Research, United States Air Force, under Contract F49620-78-C-0062.

Flow Research Report No. 162
May 1980

SECURITY CLASSIFICATION OF THIS PAGE (When Data Entered)

REPORT DOCUMENTATION PAGE		READ INSTRUCTIONS BEFORE COMPLETING FORM
1. REPORT NUMBER AFOSR-TR- 80-0473	2. GOVT ACCESSION NO. AD-A086 831	3. RECIPIENT'S CATALOG NUMBER FLOW-FR-162
4. TITLE (and Subtitle) VISUALIZATION STUDY OF TURBULENT SPOTS		5. TYPE OF REPORT & PERIOD COVERED INTERIM 1 May 1978 - 30 April 1980
		6. PERFORMING ORG. REPORT NUMBER
7. AUTHOR(s) Mohamed Gad-el-Hak and James J. Riley		8. CONTRACT OR GRANT NUMBER(s) F49620-78-C-0062
9. PERFORMING ORGANIZATION NAME AND ADDRESS Flow Research Company/Flow Industries, Inc. 21414 - 68th Avenue South Kent, Washington 98031		10. PROGRAM ELEMENT, PROJECT, TASK AREA & WORK UNIT NUMBERS 61102F 2307A2
11. CONTROLLING OFFICE NAME AND ADDRESS Air Force Office of Scientific Research Bolling Air Force Base, Building 410 Washington, D.C. 20332		12. REPORT DATE May 1980
		13. NUMBER OF PAGES 57
14. MONITORING AGENCY NAME & ADDRESS(if different from Controlling Office)		15. SECURITY CLASS. (of this report) Unclassified
		15a. DECLASSIFICATION/DOWNGRADING SCHEDULE

16. DISTRIBUTION STATEMENT (of this Report)

Approved for public release; distribution unlimited.

17. DISTRIBUTION STATEMENT (of the abstract entered in Block 20, if different from Report)

18. SUPPLEMENTARY NOTES

19. KEY WORDS (Continue on reverse side if necessary and identify by block number)

Turbulent Spots; Laminar-Turbulent Transition; Flow Visualization; Entrainment; Growth by Destabilization; Polymer Effects; Stratification Effects; Wave Packet.

20. ABSTRACT (Continue on reverse side if necessary and identify by block number)

An investigation of turbulent spots evolving in a laminar boundary layer has been conducted during the period 1 May 1978 - 30 April 1980. A flat plate was towed through an 18 m water channel. The plate was mounted under a carriage that was towed at a constant velocity. The carriage rides on a continuously replenished oil film giving a vibrationless tow.

Unclassified

20. (Cont.)

Turbulent spots were initiated by a solenoid valve that ejected a small amount of water through a hole located downstream from the leading edge.

A novel visualization technique has been employed that utilizes fluorescent dye excited by a sheet of laser. Some aspects of entrainment and strucutre of turbulent spots were inferred from the present experiments. In particular, the present results strongly suggest that another mechanism, in addition to entrainment, is needed to explain the lateral growth characteristics of the turbulent zone defining the spot. This mechanism, termed "*growth by destabilization*," appears to be a result of the turbulence in the spot destabilizing the unstable laminar boundary layer in the neighborhood of the spot.

Two additional tasks were carried out as part of this investigation. The first, a theoretical study of three-dimensional wave packets; and the second an investigation of the effects of drag reducing polymers and stratification on turbulent spots.

Flow Research Report No. 162
May 1980

Visualization Study of Turbulent Spots*

By

Mohamed Gad-el-Hak

and

James J. Riley

Flow Research Company

Kent, Washington 98031

Foreword

During the period May 1, 1978 - April 30, 1980, the United States Air Force Office of Scientific Research sponsored a research program at Flow Research Company to study turbulent spots. The work done to-date could be divided into three distinct projects. First, a visualization study of turbulent spots in a laminar boundary layer on a flat plate; second, a theoretical study of three-dimensional wave packets in a laminar boundary layer; third, an investigation of the effects of drag reducing polymers and stratification on turbulent spots. Lt. Col. Lowell Ormand was the program manager at AFOSR during most of the study period. The National Aeronautics and Space Administration, Ames Research Center, provided partial support for the second project (monitored by Dr. Anthony Leonard), and the third project (monitored by Dr. Gary Chapman).

The team at Flow Research was assisted by Dr. Mike Gaster of the National Maritime Institute, England, who carried on the second project, and by Professor Ron Blackwelder of the University of Southern California.

The present work was presented at the International Union of Theoretical and Applied Mechanics Symposium on Laminar-Turbulent Transition, held at the University of Stuttgart; at the 1979 Annual Meeting of the Division of Fluid Dynamics, American Physical Society, held at the University of Notre Dame; at Stanford University; at NASA-Ames Research Center; at the University of Washington; at Flow Research/ Boeing Seminar; and at the Pacific Northwest Section of the AIAA First Annual Mini-Symposium. Private communications were held with the world renown experts on transition including Drs. B. Cantwell, D. Coles,

S. Corrsin, R. Kaplan, P. Klebanoff, S. Kline, J. Laufer, M. Morkovin, W. Reynolds and I. Wygnanski. The present work has been received very favorably by the scientific community.

Two publications resulting from the present work were included in our renewal Proposal No. 8028. The first appeared in the Bulletin Am. Phy. Soc. 24, p. 1142, 1979, and the second is to appear in the Proceedings of the IUTAM Symposium on Laminar-Turbulent Transition, Springer-Verlag, 1980. A paper is now under preparation and will be submitted shortly to the Journal of Fluid Mechanics. Flow Research Note No. 182, entitled "Effects of Stratification and Drag Reducing Polymers on Turbulent Spots," has been completed and will be sent to AFOSR with this report.

Flow Research Films No. 40, 41 and 47 were produced to summarize some of the present visualization experiments. The first two were sent to Lt. Col. Ormand, and the third will be sent to AFOSR with this report.

The authors would like to acknowledge the valuable help of their colleagues at Flow, especially R. Metcalfe, E. Murman, D. Peecher, R. Srnsky and M. Weissman. We would also like to thank Dr. H.-T. Liu for sharing with us his recently developed dye layers visualization method.

Table of Contents

Executive Summary

Predicting and/or controlling transition from a laminar to a turbulent flow is of great practical importance. The improved design of airfoils, compressors, diffusers, etc., requires knowledge of turbulence and transition. Despite the considerable efforts spent on the study of transition, today it remains an unpredictable phenomenon. Flow Research Company carried on the present study in the hope of furthering our understanding of turbulence and transition. The study can be divided into three distinct projects: first, a visualization study of turbulent spots in a laminar boundary layer on a flat plate; second, a theoretical study of three-dimensional wave packets; and third, an experimental investigation of the effects of drag-reducing polymers and stratification on turbulent spots.

In the first project, a major effort was directed towards visualizing turbulent spots in greater detail than has ever been done. This was accomplished by using novel flow visualization techniques. Turbulent spots were initiated in a laminar boundary layer on a nominally zero-pressure gradient flat plate. The flow field was unique in that the plate was towed at 40 cm/sec through an 18 m water channel. The 191 cm-long plate had an elliptical leading edge, and the stagnation point was controlled by a trailing edge flap. The plate was mounted under a carriage that was towed at a constant velocity. The carriage rides on a continuously replenished oil film giving a vibrationless tow. The equivalent freestream turbulence was roughly 0.1 percent. When undisturbed, the boundary layer remained laminar over the entire plate.

Turbulent spots were initiated by a solenoid valve that ejected a small amount of water through a 0.5 mm diameter hole located 33 cm downstream from the leading edge. The displacement thickness Reynolds number at the ejection hole was 625.

A novel visualization technique was employed that utilized fluorescent dye, i.e., dye which is only visible when excited by a strong light source of the appropriate wavelength. Several thin dye layers were laid prior to towing the plate. These layers remained thin (about

1 mm thickness) due to the inhibition of veritcal motion caused by a weak saline stratification in the tank. Various colors were used in alternate layers to emphasize the contrast of different elevations and subsequent motion within the spot. The layers were approximately 1 cm apart, and remained quiescent until disturbed by the spot on the towed plate. Fluorescent and regular dye could also seep into the laminar boundary layer through conventional spanwise slots that were 0.15 mm wide.

The fluorescent dye was made visible by using sheets of Argon laser light which could be projected perpendicular to each of the three axis as required. The light sheets were approximately 1 mm thick, which was sufficient to resolve the large structure of the turbulent spot. Films were taken of the spots when viewed from angles that were typically perpendicular to the light sheets.

Several interesting phenomena were discovered during the course of the present study. Large amplitude wave-like structures were observed near the wall at the front boundary of the spot, with a wavelength comparable to the boundary layer thickness. Oblique wave packets were observed near the wing tip of the spot, with a wavelength several times the boundary layer thickness.

A new mechanism to explain the augmented spanwise growth of a turbulent spot was pointed out, and termed "*growth by destabilization.*" This mechanism is quite different from the classical concept of entrainment. For example, it does not involve diffusion of vorticity nor turbulent mixing. This mechanism appears to be general for all turbulent regions embedded in nonturbulent, unstable vortical flows.

In the second project, a linear theory for the development of a localized disturbance in parallel and non-parallel flows was developed. Solutions for the three-dimensional wave packet using both ray theory and direct summation of the integral were obtained. Attempts were also made to formulate the weakly non-linear theory.

In the third project, the effects of drag-reducing polymers and stratification on tubulent spots were investigated experimentally. A series of flow visualization experiments and subsequent data analysis were completed. The experiments confirmed that the polymer effects are closely associated with wall phonomena. For while the addition of polymer seems to modulate the growth by destabilization mechanism, it does not seem to affect the vertical entrainment mechanism. The stratification, on the other hand, inhibits the vertical growth of the turbulent spot.

1. Introduction

The present study is aimed at improving our understanding of turbulence and transition. The investigation is divided to three tasks: (1) visualization study of turbulent spots evolving in laminar boundary layer; (2) theoretical study of three-dimensional wave packets in a laminar boundary layer; (3) experimental investigation of the effects of drag-reducing polymers and stratification on turbulent spots.

Turbulent spots were initiated in a laminar boundary layer on a nominally zero-pressure gradient flat plate through an 18 m water channel. The plate had an elliptical leading edge, and the stagnation point was controlled by a trailing edge flap. The plate was mounted under a carriage that was towed at a constant velocity. The carriage rides on a continuously replenished oil film giving a vibrationless tow.

Turbulent spots were initiated by a solenoid valve that ejected a small amount of water through a hole located downstream from the leading edge. The displacement thickness Reynolds number at the ejection hole was 625.

A novel visualization technique was employed that utilized fluorescent dye, i.e., dye which is only visible when excited by a strong light source of the appropriate wavelength. Several thin dye layers were laid prior to towing the plate. These layers remained thin (about 1 mm thickness) due to the inhibition of vertical motion caused by a weak saline stratification in the tank. Various colors were used in alternate layers to emphasize the contrast of different elevations and subsequent motion within the spot. The layers remained quiescent until disturbed by the spot on the towed plate. Fluorescent and regular dye could also seep into the laminar boundary layer through conventional spanwise slots. The fluorescent dye was made visible by using sheets of Argon laser light which could be projected perpendicular to each of the three axis as required.

A brief history of the problem is presented in Section 2. The experimental approach is described in Section 3, and the experimental results are summarized in Section 4. Section 5 documents the theoretical study of wave packets. Finally, conclusions are stated in Section 6.

2. Brief History

The process of transition on a flat plate at zero incidence has been subjected to numerous intensive investigations. It was first studied by Burgers (1924), van der Hegge Zijnen (1924), and later, in greater detail, by Dryden (1934, 1936 and 1939). Near the leading edge, the boundary layer is always laminar, provided there is no separation, and it becomes turbulent further downstream. The critical Reynolds number at which transition takes place can be increased by reducing the turbulence intensity in the freestream. Early work on transition considered only the initial growth of infinitesimal disturbances superimposed on the laminar undisturbed flow. The theoretically predicted growth rate was confirmed experimentally by Schubauer and Skramstad (1948). When a small disturbance is applied to a laminar flow for which the Reynolds number exceeds a critical value, the disturbance initially grows exponentially with time. As the disturbance amplitude increases, the finite velocity fluctuations transport appreciable momentum. The associated Reynolds stress modifies the mean flow so that the transport of energy from the mean flow to the disturbance is modified, and the disturbance growth rate is affected. Schubauer and Skramstad showed that transition is preceded by the appearance of weak oscillations as predicted by the linearized theory of laminar instability, provided that all sources of external disturbance are sufficiently small. Those oscillations were initially in the form of two-dimensional instability waves, with wave speed about one-third of the freestream velocity, and wave length several times the boundary layer thickness. Those waves are now commonly called Tollmien-Schlichting waves in honor of the developers of the linear stability theory.

Emmons (1951) was the first to report the existence of turbulent spots created randomly as the boundary layer undergoes transition. Emmons, on the basis of visual observation in a water table, concluded that randomly generated spots grow uniformly and act independently of one another as they are swept downstream by the flow. The experiments of Tani and Hama (1953), Mitchener (1954), Schubauer and Klabanoff (1956), Hama, et al. (1957) and others confirmed that the transition phenomenon in a boundary layer is characterized by the intermittent appearance of turbulent spots which grow and move downstream with the fluid.

Dhawan and Narasimha (1958) studied the intermittency factor for transition on a flat plate, and asserted that the occurrence of turbulent spots plays a fundamental role in the mechanics of boundary layer transition, and probably also in the breakdown of a laminar motion in general. Klebanoff and Tidstrom (1959) showed the progression of events by which Tollmien-Schlichting waves evolve into turbulence. The primary stage is governed by the two-dimensional linear stability theory. The second stage involves strong three-dimensional effects, and later finite amplitude effects become important. The last stage involves the generation of turbulent spots.

Elder (1960) used dye to visualize the turbulent spots. He observed a point-like breakdown, in which the spots originate from a very small volume within the boundary layer. He investigated the conditions required for breakdown to turbulence, and the degree of interaction between adjacent spots. Elder concluded that breakdown is determined by local conditions, and is essentially independent of the Reynolds number and boundary layer thickness. A critical Reynolds number is only required in order to amplify small disturbances, whereas sufficiently strong disturbances may burst into turbulence almost instantaneously regardless of the Reynolds number. Thus, the Reynolds number becomes merely an indicator for the amplification of natural disturbances rather than a criterion for the existence of turbulence. Elder observed the interaction between two artifically generated spots which were displaced laterally, and concluded that there was no noticeable alternation in the growth rate of one spot owing to the presence of the other. Thus, he verified a major assumption in Emmons' model for the statistical properties of the spots.

Kovasznay, et al. (1962) mapped the region of concentrated vorticity in a boundary layer prior to breakdown. The total length of the region in which the vorticity exceeds the value obtained in a Blasius boundary layer was found to be approximately four times the boundary layer thickness. Klebanoff, et al. (1962) carried on an extensive experimental investigation to reveal the nature of the motions in the nonlinear range of boundary layer instability and the onset of turbulence. They introduced three-dimensional disturbances under controlled conditions in a two-dimensional boundary layer on a flat plate. They showed that longitudinal vortices are associated with the nonlinear three-dimensional wave motion, and demonstrated that the actual breakdown of the wave motion into turbulence is a consequence of a new instability which arises in the three-dimensional wave motion.

Experimental observations with flow visualization techniques suggest that the amplification of Tollmein-Schlichting waves becomes associated at some stage with the concentration of vorticity along discrete lines, which subsequently distort into vortex loops in the boundary layer. The vortex loops themselves go through a process of distortion and extension, finally resulting in the creation of spots of turbulence. Once created, these spots are swept along with the mean flow, growing laterally as well as axially with laminar flow in their trail. The spots originate in a more or less random fashion and increasingly overlap as they enlarge during their transit downstream. Finally the spots cover the entire plate, and result in fully turbulent motion. Passage of the spots over points on the surface result in alternations of laminar and turbulent flow.

Offen and Kline (1974) used flow visualization techniques to observe the turbulent boundary layer over a flat plate. They injected dye from a wall slot and from a Pitot probe; they also used a normal hydrogen-bubble wire. They showed that each lift-up is associated with a disturbance which originates in the logarithmic region, and is characterized by a mean motion towards the wall. Such disturbances are generated by the interaction of an earlier burst from further upstream, with the fluid motion in the logarithmic region.

Coles and Barker (1975) made some exploratory measurements of flow in a turbulent spot. They concluded that a turbulent spot is essentially a single large horseshoe vortex structure, and that the spot grows not only by entraining irrotational fluid from the ambient freestream, but also by entraining fluid from the ambient laminar boundary layer.

Perhaps the most thorough investigation into the kinematics of turbulent spots was done by Wygnanski, et al. (1976). They artifically initiated turbulent spots in a laminar boundary layer, and used conditional sampling methods to get the average shape of a spot, and the mean flow field in its vicinity. They showed that fluid deep in the laminar boundary layer overtakes the rear interface of the spot, and is entrained into it. Fluid outside the boundary layer passes over the ridge of the spot and is entrained through the leading interface. Their description differed slightly from the U-shaped vortex previously ascribed to the turbulent spot. Zilberman, et al. (1977) extended the Wygnanski, et al. work to track the structure of the turbulent spot as it merges and interacts with a natural turbulent boundary layer generated by a row of spherical trips. A spark was used to initiate and mark in time a turbulent spot in an initially laminar boundary layer. They showed that the spot structure tracked in the turbulent boundary layer shows a logical evolution of flow pattern, retains its identity, and suffers a negligible loss of intensity. The structure is characterized by a convection speed of $0.9\ U_\infty$. It exhibits features in detailed agreement with those of the outer region of the turbulent boundary layer and is consistent with existing two- and three-point space-time correlations. The structure shows temporal sequences similar to those obtained using flow visualization when the flow pattern is represented in a coordinate system traveling with the structure.

Cantwell, et al. (1978) conducted laser-Doppler velocity measurements for the flow in the plane of symmetry of a turbulent spot. Their measurements suggest that strong entrainment occurs along the outer part of the rear interface and also in front of the spot near the wall, while the outer part of the forward interface is passive. The experimental investigation of Wygnanski, et al. (1979) in the region following the passage of a turbulent spot in a laminar boundary layer revealed the existence of a pair of oblique Tollmien-Schlichting wave packets. The breakdown of this ordered motion into a new turbulent spot was accompanied by the appearance of an intense shear layer inclined to the wall.

More recently, Van Atta and Helland (private communication) conducted exploratory measurements of temperature fluctuations to study the structure of turbulent spots generated on a fully heated flat plate. They addressed a number of questions that have been raised by previous investigators regarding the mechanism by which a turbulent spot mixes the fluid in the boundary layer to transfer momentum and scalar properties during transition.

An important aspect of the turbulent spot, and indeed all such regions of localized turbulence, is the process by which the spot grows, incorporating previously nonturbulent fluid. Entrainment accounts for the spread of the spot normal to the plate, in a similar way that a turbulent boundary layer entrains previously irrotational fluid. Near the plate, the exterior fluid is rotational, and the growth mechanism there might be different from classical entrainment. Charters (1943) was the first to note that the transverse growth rate of a turbulent region embedded in an unstable laminar boundary layer is significantly larger than usual turbulent entrainment rates. He called this process "transverse contamination" and noted that it was independent of the originating cause. Corrsin and Kistler (1955) suggested that the spreading of a turbulent shear region into a shearing laminar region might be governed by a different propagation mechanism than that governing the spreading of turbulence into an irrotational fluid. They speculated that a destabilization of the already rotational flow could occur in addition to a transmission of random vorticity by direct viscous action (entrainment). Morkovin (1969) noted that the transverse contamination process discovered by Charters (1943) has enjoyed only one serious attention (Schubauer and Klebanoff; 1956).

3. Experimental Approach

3.1 Towing Tank System

The flat plate used in the present experiment was towed at 40 cm/sec through a towing tank that is 18 m long, 1.2 m wide, and 0.9 m deep. The flat plate was rigidly mounted under a carriage that rides on two tracks mounted on top of the towing tank. During towing, the carriage was supported by an oil film which insured a vibrationless tow, having an equivalent freestream turbulence of about 0.1 percent. The carriage was towed with two cables driven through a reduction gear by a 1.5 Hp Boston Ratiotrol motor. The towing speed was regulated within an accuracy of 0.1 percent. The main frame supporting the tank could be tilted and leveled by adjusting four screw jacks. This feature was essential for smooth operation of the carriage, whose tracks are supported by the main frame. The towing tank was designed so that flow visualizations can be made from the top, sides, bottom and ends. The bottom and side walls are made of 19 mm thick plate glass with optical quality. The end walls are made of 38 mm thick Plexiglas.

3.2 Model and Test Conditions

The flat-plate model used in the present experiment is sketched in Figure 1. It was made of Plexiglas and is 191 cm long and 107 cm wide. The deviation of the plate from flatness is nowhere greater than 0.2 mm. Care was taken to avoid leading edge separation and premature transition by having an elliptic leading edge and an adjustable lifting flap at the trailing edge. The flap was adjusted so that the stagnation line near the leading edge was located nearer the working surface.

Turbulent spots were initiated by a solenoid valve that ejected a small amount of fluid from a 0.5 mm diameter hole located 33 cm downstream of the leading edge. A square wave pulse having a 33 msec period triggered the solenoid valve. The injected fluid created a three-dimensional disturbance, mostly a vortex ring, which triggered a localized transition to turbulence. The Reynolds number based upon a towing speed of 40 cm/sec, and the displacement thickness at the injection hole was 625, well above the absolute limit of instability.

The boundary layer on the working surface remained laminar until tripped close to the trailing edge. The plate was positioned 5 cm from the tank walls, and the circulation around the plate generated by the flap was such that disturbances were not communicated from the bottom surface to the top (working) surface.

3.3 Flow Visualization

The turbulent spots were made visible by novel techniques which utilized fluorescent dye, i.e., dye which is only visible when excited by a strong light source of the appropriate wavelength. This provided an extra degree of freedom in observing the flow because both the dye and light location could be controlled within the limitation of the experimental apparatus. A 5-watt argon laser (Spectra Physics, Model 164) was used with a cylindrical lens to produce a sheet of light that could be projected perpendicular to each of the three axis as required. The light sheets were approximately 1 mm thick, which was sufficient to resolve the large structure within the turbulent spot.

Two different methods of dye injection were employed. In the first, the dye seeped into the laminar boundary layer through a 0.15 mm wide, 30 cm long spanwise slot. The slot was milled at a 45^{o} angle to minimize the flow disturbance and was located 25 cm downstream of the leading edge. The slot was divided into four separate sections so the spanwise diffusion of turbulent fluid with different dyes could be studied. The dye remained near the plate surface until the turbulent spot caused it to lift and diffuse. Sheets of light along all three axis provided striking structural details.

Dye was also placed in the flow field by laying several thin, horizontal sheets prior to towing the plate. These layers remained thin, about 1 mm thick, due to the inhibition of vertical motion caused by a weak saline stratification in the tank. Fluorescein, Rhodamine-B, and Rhodamine-6G dyes were used which fluoresced green, dark red and yellow, respectively, when excited by the argon laser. In a flood light, the first two dyes fluoresced green and dark red, but Rhodamine-6G had a faint red color. The alternating sheets of different colors remained quiescent until disturbed by the turbulent spot on the towed plate. The motion of the potential flow could also be observed since dye layers existed there also.

The visualization information was obtained using 35 mm photographs and 16 mm cine films. The cameras were typically controlled by micro-switches which filmed the spot at predetermined times after its generation. The 16 mm films were analyzed by a stop-action projector.

3.4 Stratification and Polymer Additives

A stratified fluid of a predetermined density profile could be made by feeding salt water, layer by layer with increasing density, into the tank through two channels along the tank bottom. The salinity of the water and its feeding rate determined the density profile in the undisturbed tank. A linear density profile is characterized by its Brunt-Vaisala frequency N , defined as:

$$N \equiv \frac{1}{2\pi}\sqrt{\frac{-g}{\rho_o}\frac{d\rho}{dy}} ,$$

where g is the gravitation acceleration,
ρ_o is a reference density (1 gm/cm^3), and
$\rho(y)$ is the undisturbed density profile.

The Brunt-Vaisala frequency provides a convenient measure of the time scale at which stratification effects are important. It is the frequency of oscillation of a fluid particle under infinitesimal perturbation. In the present experiment, N varied in the range 0-0.7 Hz.

The polymer used in the present experiment was Polyox, WSR-301 (polyethylene oxide) manufactured in powder form by Union Carbide Corporation. It has a molecular weight of about 4×10^6, and was used in concentration of 50 particles per million (ppm) by weight. Good initial dispersion of the Polyox resin in the towing tank water is necessary for good dissolution. If the resin powder is not properly dispersed, the partially dissolved, wetted particles will agglomerate and form gels which will dissolve only with prolonged high speed agitation. However, such prolonged high speed agitation must be avoided to prevent shear degradation of the resin. A novel method was used in the present study to dissolve the polymer in the water. An aspirator driven by 80-psi compressed air was used to lift the polymer from its container into a 25-mm PVC pipe. The pipe released the mixture of air and polymer near the bottom of the towing tank. The air provided an ideal media for dispersing the resin. The polymer mixed well with the water without forming gels, and the air escaped to the surface.

4. Results and Discussion*

4.1 Spot Structure

Several reference runs were made to check the overall quality of the towing system and the established flow field. Conventional food coloring dye was allowed to seep from the spanwise slot and several holes near the leading edge. Dye seeping from the leading edge holes indicated that the stagnation point was slightly toward the working side of the plate and no separation occurred. When unperturbed, the dye from the slot remained on the surface and had a glassy smooth appearance over the entire length of the plate, indicating that a laminar boundary layer was maintained until the end of the plate, at which the Reynolds number was $U_\infty x/\nu = 7.6 \times 10^5$, for a towing speed $U_\infty = 40$ cm/sec. When disturbed by the solenoid injection of fluid through the hole at $x = 33$ cm, a spot having the classical arrowhead shape could readily be observed as the turbulence removed the dye from the wall layer. The developing shape of several spots was mapped to determine the virtual origin. It occurred at $x = 43 \pm 2$ cm, i.e., 10 cm downstream of the ejection hole, and at $t = 0.63 \pm 0.1$ sec after the ejection.

A plan view of the turbulent spot moving from left to right is shown in Figure 2. The fluorescent dye was injected uniformly through the spanwise slot, and was made visible by a sheet of laser light located at $y \simeq 0$. As the spot develops, the random turbulent motion removed dye from the wall and elevated it above the plate. Since the light sheet is slightly thicker than the dye layer on the plate, both the dye in the laminar boundary layer and the dye near the wall within the spot were visible. The light illumination was from both sides of the figure. Some absorption of the light occurs and the sheet loses intensity in the spanwise direction. Consequently the sides appear brighter than the interior. The general arrowhead shape of the spot is clearly evident. Some evidence of the streamwise streaky structure at the rear of the spot is seen in the figure. However, since little dye remained at this location after the passage of the spot, this aspect of

---

*Portions of this section were written with the help of Professor R. Blackwelder.

the motion was more easily seen using conventional flood lights which provided an integrated view and hence more contrast. This suggests that the streaks are made visible by coagulating the dye into thin sheets in the x-y plane, consistent with the concept of counter-rotating streamwise vortices discussed by Cantwell, et al. (1978).

Several runs were taken using different elevations of the sheet of light. As the height of the sheet increased, individual turbulent eddies inside the spot became more discernible and their scale in the streamwise and spanwise directions increased. A sequence of views in the x-z plane are shown in Figure 3. The height of the light sheet was 1.3 cm above the plate, making the height almost twice the undisturbed laminar boundary layer thickness at this location ($\delta_\ell \simeq 0.7$ cm) . The elapsed time since the spot was generated is shown on the right, and for reference a scale of the physical dimensions is shown. Some turbulence may exist between the dyed modules seen in the figure, since the dye only tags that fluid which was originally near the wall. Nevertheless, this sequence and films of the x-y cross-section of the spot (see Figure 5) clearly show well-mixed turbulent eddies moving away from the wall. Most striking is that at this elevation, the growth occurs at the rear of the spot with very little new turbulence appearing near the head. That is, first several turbulent eddies appeared. As the flow field developed, it was apparent that these eddies were near the head of the spot and they remained relatively coherent until swept from the field of view. As seen in the figure, the spot grows by the appearance of more eddies. However the new eddies typically occur only upstream of the existing ones, i.e., towards the rear of the spot. This is consistent with Cantwell, et al. (1978) assertion that strong entrainment occurs along the outer part of the rear interface. Our data do not confirm a conclusion reached by Wygnanski, et al. (1976), that there is appreciable entrainment along the outer front boundary of the spot. There was a slight tendency for the turbulent eddies to appear first near the wingtips and later in the middle of the spot. This may have been a manifestation of the visualization technique, since the earlier passage of the head of the spot would have left less dye for tagging the turbulence in the interior. The scale of the turbulence eddies at this elevation within the spot is roughly a turbulent boundary layer thickness in the streamwise and spanwise directions.

An example of the ingestion of the vortical laminar fluid near the wall into the spot is seen in Figure 4. Fluorescein dye was allowed to seep from the spanwise slot and occupy the wall region. The sheet of light positioned at $y \simeq 0.1$ cm illuminated the spot as soon as the turbulence was present. The nose of the spot was 160 cm downstream of the ejection hole. A single dye line at $y = 0.1$ cm was also present and can be seen ahead of the spot. As the spot overtakes the dye line, a strong, large amplitude wave-like structure was observed. In this view, a Tollmien-Schlichting wave would be visible only if it had a velocity component along its crest to distort the dye line. Thus if the observed motion is a wave, it must be oblique, although the angle cannot be determined from the single dye line. The wavelength in the streamwise direction measured from the figure is approximately $\lambda_x \simeq 1.2$ cm, compared with the laminar boundary layer thickness at this location of approximately 1 cm. A point of constant phase was observed to move downstream at roughly $U_\infty/3$, and hence was rapidly overtaken by and ingested into the spot. Presumably these structures might have existed even further upstream of the spot, but were not visible until their amplitude became very large. An earlier sequence in this film from which Figure 4 was extracted illustrated a strong spanwise velocity near the wingtip before the spot was large enough to intersect the dye line. As the spot continued to expand outward, the dye line was also moved outward near the wingtip in agreement with the outward velocity component measured by Wygnanski, et al. (1976). Slightly later, the spot was large enough that it began ingesting the dye line as discussed above.

A different view of the spot is found in Figure 5. The pre-existing horizontal dye sheets were illuminated primarily by the light sheet in the x-y plane, however the dye also reflected some room lighting. On the original films and photos, this room-lit dye provided a convenient reference line from which the disturbed motion could be compared. The sheet of light could be placed at different spanwise locations, providing cross-sections of the spots at different z-positions. The example in Figure 5a is taken on the centerline, and 5b is taken at 6 cm (approximately $10\delta_\ell$) off center. The outline of the spot in this view is highly contorted at all spanwise locations. The general shape and aspect ratio of the spot agrees with the conditionally averaged shape of Wygnanski, et al. (1976) and Cantwell, et al. (1978). However, no single dominate eddy was observed at any spanwise location. Instead the spot contained many eddy structures having streamwise length and height scales of typically a turbulent boundary layer thickness δ_t. As seen in the figure, they have a preferred inclination in the downstream direction. These eddies seemed to be independent of each other; in fact, the interior of the spot at all spanwise locations resembled a turbulent boundary layer. The eddies slowly grew and moved away from the plate, thus providing the growth in the normal direction as observed in Figure 3.

The different colors in the dye layers allowed one to observe the turbulent entrainment and mixing in some detail. Most of the observable entrainment occurred on the back of the spot, as reported by Cantwell, et al. (1978). Although "nibbling" may be important in the later stages, the most obvious mechanism was that of "gulping", i.e., large parcels of irrotational fluid being ingested into the boundary layer between two eddy structures. Examples of this are seen in Figure 5 where the potential fluid extends deep inside the turbulent region. Similar conclusions have been drawn by Falco (1977) for a fully developed turbulent boundary layer at moderate Reynolds numbers.

The effects of the spot are felt over a large domain in the irrotational region. For example, even though the outermost dye layer in Figure 5a is located at $2\delta_t$, it is observed to have been displaced at least 0.5 cm $(0.2\delta_t)$ as the spot passes underneath. This agrees with the strong correlation of the normal velocity component into the potential region, which was reported by Blackwelder and Kovasznay (1972) in a turbulent boundary layer. In front of the nose, the dye lines at $y \simeq \delta_t$ have been displaced downward, indicative of the strong normal velocity component reported by Wygnanski, et al. (1976). Closer to the turbulent eddies, stronger distortions are observed as the irrotational fluid is marked for entrainment.

A cross-section of the spot in a plane perpendicular to the mean flow is shown in Figure 6. Although the laser sheet was aligned in the y-z plane, the camera was by necessity outside the towing channel; thus the view is from a 45^{o} oblique angle. The view in Figure 6 is approximately half-way between the nose and tail of the spot. The spot again appears to be composed of a random collection of turbulent eddies as illustrated by Figures 3 and 5. The most impressive feature from this angle was a strong motion perpendicular to the wall which can be inferred from the dye line displacement slightly outside the spot. In the irrotational region, a motion toward the wall is seen directly above the tip of the spot. A little further out in the spanwise direction, a large upward displacement is observed in the laminar boundary layer. Wygnanski, et al. (1976) measured the normal velocity at $y/h_o = 0.3$ (h_o is maximum height of the spot). They observed a component toward the wall at the edge of the spot, but did not make measurements in the vicinity of the positive normal velocity.

Careful viewing of the movie sequence from which Figure 6 was extracted revealed no strong evidence of a predominant vortical structure. The spot dynamics seemed to be controlled by individual, independent eddies, in much the same way as the case of a turbulent boundary layer.

4.2 Lateral Growth

One interesting and important aspect of the turbulent spot is the process by which it grows, incorporating previously nonturbulent fluid. From the previous discussion and the work of others, e.g., Wygnanski, et al. (1976) and Cantwell, et al. (1978), it is apparent that the spread of the spot normal to the plate is mainly due to classical entrainment, in much the same way that a turbulent boundary layer entrains previously irrotational fluid. This process was first studied by Corrsin & Kistler (1955) in typical turbulent shear flows. Some of the most distinctive features of the classical concept of entrainment (see Townsend; 1976) are:

1. The turbulent region is separated from the nonturbulent region by a distinct interface.
2. The interface thickness has been speculated to be of the order of Kolmogorov length scale $(\nu^3/\varepsilon)^{1/4}$ (Corrsin & Kistler; 1955).

3. The turbulent region is characterized by random three-dimensional vortical flow; the nonturbulent fluid is irrotational.
4. The process of entrainment must ultimately be by direct contact, i.e., by the local diffusion of vorticity. This is followed by a rapid increase in vorticity due to local straining.
5. If a passive scalar is introduced into the turbulent region, it will serve as an effective marker of that region (e.g., Fiedler & Head, 1966; Chen & Blackwelder, 1978).

There is strong reason to believe that the turbulent spot does not spread parallel to the plate by classical turbulent entrainment. First of all, the exterior fluid, being in the laminar boundary layer, is highly rotational; second, it is also unstable. Therefore, feature 3 above does not hold, and it is not necessary that the turbulent region spread through direct contact (feature 4). The question is then, what process controls the spreading? Is it the classical entrainment process, or is some other mechanism at work? If different, how is it different both qualitatively and quantitatively? The answers to these questions are critical for understanding the spread of a spot, and more generally, transition.

Some rough estimates can be made to indicate that there may be a new mechanism present. Let us compare the growth rates of the spot in the normal and spanwise directions. Let h denote the characteristic scale in the direction perpendicular to the wall. In a turbulent boundary layer, h grows like $x^{0.8}$, very close to the linear growth rate in the spot as found by Cantwell, et al. (1978). Using their similarity transformation, the growth rate of h is $dh/dx \simeq 0.013$. On the other hand, the growth rate of the characteristic scale, b, in the spanwise direction can be estimated from the maximum angle subtended by the spot measured from its virtual origin. Using the typical value of 10° as reported by Wygnanski, et al. (1976), yields $db/dx \simeq 0.18$. Thus the spanwise growth is more than an order of magnitude greater than the classical entrainment growth in the normal direction. This fact is suggestive of an additional mechanism, but is by no means conclusive.

A series of visualization experiments were performed to better elucidate the lateral growth mechanism. Dye was used as a passive scalar contaminant to mark the initially turbulent fluid. If turbulence were only acquired by entrainment, the dye would continue to diffuse and mark the entire turbulent region, in a manner similar to the smoke and heat used respectively by Fiedler & Head (1966), and Chen & Blackwelder (1978). Alternatively, if additional turbulence were acquired by mechanisms other than classical entrainment, the spot would not be dyed the same color as the initial region. In one experiment, blue dye was injected from the solenoid valve in order to mark the initial patch of turbulence, and red dye was emitted through the slot in order to mark all the turbulence within the spot. Movies of the plan view of the turbulent spot indicated that the original turbulent region, dyed blue, did not spread nearly as fast as the spot. In other words, new turbulent fluid was incorporated into the spot without being tagged with blue dye.

To further explore the diffusive properties of the spot, the dye slot was partioned into four independent regions, and different dyes were used in each slot. The movie records showed clearly that the spanwise diffusion of dye across the sections is much less than the spanwise growth rate of the spot. Estimates of the dye diffusion obtained from the films indicate that the spanwise diffusion was comparable to diffusion in the normal direction, i.e., the turbulent boundary layer growth rate.* Although the diffusion of dye proceeds at the same rate as entrainment in the normal direction, diffusion and spot growth have markedly different rates in the lateral direction. Townsend (1976) points out that the entrainment rate of a turbulent boundary layer is much less than that of a jet or wake, so that one could argue that the classical entrainment mechanism with different rates could account for the contrasting growth rates in the normal and spanwise directions. However, in the classical concept of entrainment, diffusion and entrainment proceed at the same rate, and the present experiment clearly shows that the lateral diffusion within the spot is significantly different than the growth rate in that direction.

To examine further the nature of the spread of a turbulent region into an unstable, laminar boundary layer, the turbulent wake behind a

---

*Similar lateral diffusion rates prevail in a fully-developed, turbulent boundary layer, since the velocity fluctuations in the spanwise and normal directions are comparable.

roughness element in a laminar boundary layer was studied. The roughness element, a circular cylinder with 0.32 cm diameter and 0.25 cm height, was placed 30 cm behind the leading edge, and the plate was towed at 30 cm/sec. The wake from the roughness was easily visualized by coating it with dye dissolved in corn syrup, as seen in Figure 7a. Figure 7b was taken under identical conditions except an additional dye was seeped through the spanwise slot. As is readily evident, the turbulence region, which is marked by the dye seeping from the slot, extends significantly outside the wake of the roughness, which is marked by the dye pasted on the roughness. The width of the turbulent region increased more rapidly and was always wider than the wake of the object initiating the wedge. In the film from which Figure 7b was obtained, an occasional spot could be observed moving downstream. It was distinguishable from the other turbulence because its wing tips extended slightly beyond that marked by the turbulent dye. The growth of the wake in Figure 7 is approximately 2°, whereas the total turbulent region grows at $6 \pm 0.5^{\circ}$. The outer region of the observed wing tips subtended a half-angle of $10 \pm 0.5^{\circ}$. Similar data have been obtained by Schubauer & Klebanoff (1956) using hot-wire measurements. Klebanoff (private communication) observed that as the Reynolds number increased, the growth rate of the total turbulent region behind the roughness approached that of the intermittent region (spots).

When the roughness element was removed and the plate towed at the same velocity, the boundary layer remained laminar over the entire surface. Whenever the roughness was located in a stable laminar boundary layer ($U_{\infty}\delta^*/\nu < 450$) , flow irregularities introduced by the cylinder were damped. Apparently not just a vortical flow, but an unstable vortical flow is a necessary condition for the lateral growth process to take place.

The above visualization experiments confirm that the augmented spanwise growth of a turbulent region embedded in an unstable laminar boundary layer may be due to a destabilization process, in which the turbulent eddies induce such a strong disturbance that the surrounding laminar flow breaks down. It would be expected that the properties of the turbulent-nonturbulent interface are different from that in the classical entrainment case.

4.3 Effects of Drag Reducing Polymers

Polyox, WSR-301 polymer was used in a concentration of 50 ppm. The flat plate was towed at 40 or 60 cm/sec, corresponding to R_{δ_*} at the injection hole of 625 or 766, respectively. The mean wall strain rate in the turbulent spot was above the onset strain rate for WSR-301, which is about 320 sec^{-1} (Berman & George; 1974). This means that drag reducing effects should be observed in the present experiment. However, the mean wall strain rate was below that necessary for the production of "polymer induced fluctuations" discovered by Bertshy & Abernathy (1977).

Figure 8 shows a plan view of a turbulent spot generated in pure water and one generated in a dilute polymer solution. Each spot is moving from left to right relative to the plate which is towed at 40 cm/sec. Fluorescent dye was injected uniformly through the spanwise slot, and was made visible by a sheet of laser light located at $y = 3$ mm. As each spot developed, the random turbulent motion removed dye from the wall and elevated it above the plate. In the movie frames from which Figure 8 was extracted, one can observe that the polymer tends to suppress the small-scale turbulent structures. Also, with the polymer additive, the lateral growth rate is reduced by about 15 percent, resulting in a more elongated spot in the dilute polymer solution. This reduction is much less pronounced than the 40 percent reduction observed by Bertshy and Abernathy (1977). It should be noted, however, that the wall strain rate in their experiment was higher than that in the present study. Moreover, because their experiments were carried out using a shallow water table, their flow extended only to y^+ on the order of 100, and polymer effects could conceivably be more pronounced in the absence of outer flow. The addition of the polymer does not seem to significantly affect other gross parameters, such as the propagation speed of the head or the tail of the spot.

One interesting result of previous experiments on turbulent spots is that, for nonaccelerated flat-plate boundary layers, the average shape of the spot appears to be independent of ambient conditions, i.e., local Reynolds number and strain-rate. Thus the lateral angle subtended by the spot has always been found to be approximately 10^o, and the growth rate normal to the wall to be approximately that of a turbulent boundary layer. This fact may provide the basis for a theoretical approach to turbulent spots. However, when the polymer is added, the lateral growth rate appears to depend on the strain-rate (and most certainly on the polymer concentration), as found from comparing our results to those of Bertshy and Abernathy (1977).

Figure 9 shows another plan view of a turbulent spot generated in the dilute polymer solution. The plate was towed at 60 cm/sec, and the sheet of laser light was located at $y \simeq 0$. The average eddy size is smaller than that depicted in Figure 8, because the cut is closer to the wall and because the Reynolds number is higher. The wall strain rate in this case is about 20 percent higher than that in Figure 8.

Several runs were taken using different elevations of the sheet of light. As the height of the sheet increased, individual turbulent eddies inside the spot became more discernible, and their scale in the streamwise and spanwise directions increased. The effect of the polymer on the spanwise growth remained about the same.

The effect of the polymer on the vertical growth of the spot was minimal, as shown in the example in Figure 10. In this figure, the dye was illuminated by a sheet of laser light in the x-y plane, located at $z = 6$ cm. The plate was towed at 40 cm/sec, and both spots are 4.2 seconds old. The head of both spots is at right. Both the spot in the pure water and the one in the dilute polymer solution seem to consist of many eddy structures having typical streamwise length and height scales of a turbulent boundary layer thickness. The eddies have a preferred inclination in the downstream direction, and seemed independent of each other. In fact, the interior of both spots at all spanwise locations resembled a turbulent boundary layer (Falco; 1977). The eddies slowly grew and moved away from the plate, providing the growth in the normal direction. No single dominate eddy was observed at any spanwise location.

Thus, it seems that the addition of polymer mainly affects the spanwise growth of a turbulent spot. This is consistent with our concept of the spot growing vertically by classical entrainment, but growing laterally by destabilization. It is known that drag reducing effects associated with polymers occur in regions of high strain-rate, e.g. near boundaries, suppressing smaller-scale motions. Thus it is likely that the stability characteristics of the laminar boundary layer are modified by the drag reducing additives, i.e., the flow is less unstable. Hence the destabilization process is somewhat inhibited, resulting in a slower lateral growth rate. A better understanding of the dependence of lateral growth rate on the local strainrate, and a determination of the effects of the polymers on the stability characteristics of the flow should thus give further insight into this lateral growth mechanism.

4.4 Stratification Effects

Turbulent spots were generated in the presence of a linear, stable density gradient having a Brunt-Vaisala frequency in the range 0-0.7 Hz. Figure 11 shows the effects of stratification on the vertical growth of a turbulent spot. The fluorescent dye was illuminated by a sheet of laser light in the x-y plane, located at $z = 0$. The plate was towed at 40 cm/sec, and both spots are 3.5 seconds old. Figure 11a shows the spot in the homogeneous fluid $(N = 0)$, and Figure 11b shows the spot in the stratified fluid ($N = 0.1$ Hz). The stratification inhibits the vertical growth of the turbulent spot. The effect is more pronounced near the head of the spot (to the right). This is expected since the head of the spot is generated first, and thus has more time to "feel" the stratification effects. The vertical turbulent motion causes vertical transport of mass, which in turn converts kinetic energy to potential energy. As a result, vertical motion is suppressed and the vertical mass transport weakens.

The stratification made it more difficult to maintain a flat sheet of laser light because of the index of refraction changes caused by the density fluctuations. In addition, a view of the turbulent spot was distorted, since the light emitted by the fluorescent dye had to pass through the fluid with fluctuations in the index of refraction. Those effects became more pronounced with the increase in the intensity of stratification $(N > 0.1$ Hz$)$. Runs conducted at progressively larger values of Brunt-Vaisala frequency were more difficult to analyze because of the distortion effects described. However, it was clear that increasing the Brunt-Vaisala frequency increased the suppression of the vertical growth of a turbulent spot.

Figure 12 shows a series of traces taken from movie frames. Run conditions were the same as that in Figure 11. Figure 12a shows a cross-sectional view in the x-y plane of a turbulent spot evolving in a homogeneous fluid, while Figure 12b shows a similar view for a spot evolving in a stratified fluid with a Brunt-Vaisala frequency 0.1 Hz. The elasped time since the spot was generated is shown on the right, and for reference a scale of the physical dimensions is shown. The head of the spot in the stratified flow began showing evidence of "collapse" at $t = 2.6$ seconds ($Nt = 0.26$, or 26 percent of a Brunt-Vaisala period). It is known that wakes in stratified fluids begin to collapse after about a quarter of a Brunt-Vaisala period (Lin and Pao; 1979). Apparently the influence of stratification on the dynamics of a turbulent spot is similar to the influence on turbulent wakes.

The stratification did not seem to affect the spanwise growth of a turbulent spot, as estimated by the maximum angle subtended by the spot measured from its virtual origin. This angle was typically 10°, the same as that for the homogeneous case. However, due to collapse, it did affect the lateral spread of the head of the spot, causing it to be somewhat wider and flatter than for the nonstratified case. It is not clear how the overall shape of an "old" spot, i.e., one that has existed for several Brunt-Vaisala periods, would be modified.

5. Development of a Wave Packet in a Growing Boundary Layer*

5.1 Introduction

The initial phase of the process of transition from a laminar to a turbulent flow involving the growth of very small disturbances is reasonably well understood for most of the flows of general interest, but the nonlinear stage of development, and particularly the final process of breakdown into turbulence, remains obscure. Most advances in the theoretical treatment of the problem have been concerned with the instability of parallel flows, since this geometrical restriction greatly simplifies the analysis by reducing the governing relations from partial to ordinary differential equations. Direct confirmation of theoretical work has not been generally possible because of experimental difficulties associated with such confined flows, and consequently most of the detailed experiments concerning the behaviour of instability waves have been carried out in boundary layers. In these developing flows disturbances first become unstable some distance from the leading edge. This allows the growth of artificially excited waves to be followed from a stable upstream location into a zone of amplification, and measurements do not become contaminated by the randomly excited natural fluctuations generated by free-stream turbulence. This situation does not arise in a parallel flow, where above some critical Reynolds number the flow is unstable at all streamwise locations and natural disturbances can develop from the entry region. The fluctuations arising from these natural sources eventually dominate the downstream flow and make it difficult to carry out experiments on controlled disturbances.

It has been observed that transition from a laminar to a turbulent flow is brought about through the amplification of vorticity waves excited by various external stimuli. An instability mechanism enables these initially very weak disturbances to amplify as they propagate downstream. At some stage the perturbations become so large that their behaviour is no longer controlled by purely the linear terms in the equations of fluid motion, and then more complex processes involving modal interactions take over. When this stage is reached it is generally

*This section is written by Dr. M. Gaster.

found that fully developed turbulent flow becomes established very rapidly. The stochastic nature of any naturally excited waves makes it very difficult to study these nonlinear processes that lead to turbulence, and for this reason recourse has often been made to experiment on simpler periodic waves that can be introduced artificially in a controlled manner.

Most significant experimental results relate to the flat plate boundary layer, where measurements have been made on periodic two-dimensional waves excited artifically by a wave maker. The earliest successful experiment of this type was carried out by Schubauer & Skramstad (1948) in a specially designed wind tunnel of very low turbulence. Their measurements of growth rates and propagation velocities were compared with the calculations of Schlichting (1935), which were based on a quasi-parallel treatment, and the substantial agreement achieved played a vital role in establishing the theory.

Unfortunately when a simple periodic wave train is generated in the flow many of the important nonlinear processes that lead to breakdown in the case of natural transition do not occur. Artificially excited isolated wavepackets, on the other hand, do incorporate the necessary modulation of the wavetrain that turns out to be so vitally important. It appears that the violent nature of breakdown observed in natural transition can be modelled in the breakdown of a wavepacket, but in a controlled manner.

Experiments on wavepackets and their breakdown to turbulence has been undertaken by Gaster & Grant (1975), and theoretical methods need to be developed to understand the information being acquired. In these experiments it has been shown that the wavecrests of the propagating wavepacket become distorted when the amplitude of the disturbances is large enough. These distortions of the wave fronts are associated with steep shear layers within the boundary layer, and it is their presence that enables the secondary instability to support the amplification of the high frequency bursts of oscillation that eventually lead to embryo turbulent spots (Gaster; 1978a). Although it is clearly outside the scope of existing theoretical techniques to predict this occurrence, it can be expected that the initially weak nonlinear phase that is the precursor of this process can be analysed. Since the observed breakdown occurs locally it seems appropriate to attempt to describe the flow prior to this event by a local rather than a global mathematical model. It is intended therefore to attempt to produce a local theoretical description of the flow structure within a wavepacket that is evolving in a slowly growing boundary layer in the regime where weak nonlinear behaviour is also taking place. The present part of this project is concerned with the linear phase of evolution in a growing boundary layer.

5.2 Formulation

Theory for periodic linear waves in a purely parallel base flow is well established, and can be used to describe more complex disturbances by a suitable superposition of these basic disturbances. A wavepacket, for example, can be described by a summation or integral of these basic waves with respect to frequency, where every component is equally represented. An evaluation of this integral can then be obtained by the method of steepest descent to provide an asymptotic representation that is valid at large distances from the origin of excitation. The resulting "ray-like" solution provides a description of the flow in any specific region of the packet. The necessary modification of this solution to cater for slow spatial growth of the mean flow as well as for weak nonlinear effects are sought. In the case of waves that are excited by a periodic source, the influence of any slow spatial development of the base flow can be found by a perturbation expansion technique about the zero-order solution obtained from the parallel flow theory. The first-order correction to the amplification rate is then found as a scaling factor, which can be obtained by a multiple expansion (Bouthier; 1972) or by an iterative procedure (Gaster; 1974). Higher terms of the resulting series expansions can, in principle, also be found. These series representations of periodic waves could of course be summed over all frequencies to form the resultant wavepacket solution that is valid in a growing boundary layer, but this seems cumbersome. In the approach used here the same idea of iteration about an asymptotic form of wavepacket given by the zero-order locally parallel flow integral is used.

To explain this approach it is necessary to discuss briefly the asymptotic form of solution for a wavepacket in a truly parallel flow, and to build on this for the case of non-parallel boundary layer. In a parallel flow, wavetrains of frequency ω can be described for a stream function

$$\psi(x,y,t) = \phi(y,\alpha,\omega)e^{i\left[\alpha(\omega)x - \omega t\right]} , \tag{1}$$

where α is the complex wave number ($\alpha_i < 0$ is unstable) . A local pulsed disturbance will excite all possible waves $\alpha(\omega)$ and the resultant motion will therefore be given by an integration in the frequency domain

$$\psi \rightarrow \int \phi\left[y,\alpha(\omega),\omega\right]e^{i\left[\alpha(\omega)x - \omega t\right]}d\omega \quad . \tag{2}$$

An asymptotic evaluation of the above can be obtained by the method of steepest descent. $\alpha(\omega)$ is expanded about a point ω^* , where the derivative of the exponent with respect to ω is zero,

$$\frac{\partial}{\partial\omega}\left[\alpha(\omega^*)x - \omega^* t\right] = 0 \;, \quad \text{at} \quad \omega^* \;,$$

or

$$\frac{\partial}{\partial\omega}\alpha(\omega^*) = \frac{t}{x} \quad . \tag{3}$$

For physically real values of x and t , ω^* is such that $\frac{\partial}{\partial\omega}\alpha(\omega^*)$ must be real and can be identified with the reciprocal of the group velocity of the wave system. Although ω^* will in general be complex, the maximum amplitude of the packet is centered on the ray with $\omega_i^* = 0$. Since the dispersion $\omega(\alpha)$ is not dependent on the observer station there will be a value of ω^* for each ray which is also independent of x. The solution for large x or t is

$$\psi = \sqrt{\frac{2\pi}{\frac{\partial^2\alpha}{\partial\omega^2}x}} \times \phi\left[y,\alpha(\omega^*),\omega^*\right]e^{i\left[\alpha(\omega^*)x - \omega^* t\right]}\left\{1 + 0\left(\frac{1}{x}\right) + \dots\right\}, \tag{4}$$

and the ray-like structure of the solution is apparent. Equations 3 and 4 shows how certain properties of the solution depend only on t/x, while the magnitude of the packet is determined by the distance from the source. This formulation has been compared with direct numerical evaluation of the integral and with other proposed asymptotic representations by Gaster (1979).

The extension of the above to situations where the boundary layer slowly grows in thickness with x, follows from the way a simple periodic wavetrain is treated in this situation. In that case the stream function for a wave can be written

$$\psi = A(x,\omega)\, e^{i\left[\int_{xo}^{x} \alpha(x,\omega)dx-\omega t\right]}\left\{\phi_o(y,x,\omega) + \frac{\phi_1(y,x,\omega)}{R}\right\}, \quad (5)$$

where the zero order term, ϕ_o, has the structure of a locally parallel flow at that Reynolds number. The weak scaling function A is defined in terms of integrals of ϕ_o and its adjoint.

The zero order component of the wave packet can thus be expressed by an integral of the form

$$\int \phi_o\ (y,x,\omega)\ e^{i\left[\int_{xo}^{x} \alpha(x,\omega)\ dx\ -\ \omega t\right]} d\omega\ .$$

For the purposes of describing the evaluation of this integral it is useful, at this stage, to follow the procedure outlined by Gaster (1979) and dispense with the vertical structure of the problem and consider the evaluation of the integral

$$I = \int e^{i\left[\int_{xo}^{x} \alpha(x,\omega)\ dx\ -\ \omega t\right]} d\omega \quad (6)$$

5.3 Evaluation of the Integral

The integral I can be evaluated by the method of steepest descent by expanding the integral about the point ω^* in the ω-plane, where the derivative of the exponent is zero.

Writing $I = \int e^{iQt}\, d\omega$, where $Q = \int_{xo}^{x} \frac{\alpha(x,\omega)}{t}\, dx - \omega$,

ω^* is chosen so that:

$$\frac{\partial}{\partial\omega} Q(\omega^*) = 0 \ .$$

Then I becomes:

$$\sqrt{\frac{2\pi}{Q''(\omega^*)x}} \times e^{iQ(\omega^*)t} \left\{ 1 + 0\left(\frac{1}{x}\right) + \cdots \right\} , \qquad (7)$$

where

$$\int_{xo}^{x} \frac{\partial}{\partial\omega} \alpha(\omega^*)\, dx = t \ . \qquad (8)$$

Thus for real x and t this definition of the integral must be a real quantity, and ω^* is therefore chosen so that the value of the integral is equal to t . Note that $\frac{\partial\alpha}{\partial\omega}$ will be real at only one point in the range of integration, unlike the situation that occurs with parallel flows. Thus for each x and t station there is a specific value of ω , ω^* that makes $\frac{\partial Q}{\partial\omega} = 0$, and provides a point about which an expansion can be obtained in the form of equation (7). Similarity with the parallel flow calculation is not quite so clear because the ray-like character along which certain properties of the solution propagate is now lost. In fact the ray concept is not especially useful here because the rays defined by equation (8) lie in the complex t-domain This arises, presumably, because of the elliptic nature of the problem, and should be kept in mind as a warning of possible difficulties if rays were to coincide. Each x and t has its associated value of ω^* defining the structure at that point and thus provides the required local solution.

5.4 Computations

The series method of defining the eigenvalues where

$$\frac{\omega}{\alpha} = \sum_{n,m} A_{nm} \left(\alpha^2-\alpha_o^2\right)^n \left(\alpha R-(\alpha R)_o\right)^m$$

was used (Gaster; 1978b). It was found possible to compute values of ω for given values of α and R very easily and quickly by this method using the previously calculated values of the A_{nm} coefficients. Speed was essential in the present exercise where enormous numbers of eigenvalues had to be evaluated. Real values of x and t were found that satisfied equation (8) for a range of ω^*. The results of this computation are displayed on Figure 13. Each value of ω^* produced one root with both x and t real. The evaluation of equation (7) was then carried out for 12 downstream locations over a range of values of t. Each point in the x-t plane involved an iterative search for the appropriate ω that satisfied (8) for real x and t.

The summation representation of the wavepacket given by equation (6) was also evaluated for the same values of x and t that had been used in the asymptotic solution. Although as yet there are no graphical representations of these two sets of results, isolated points that have been compared show excellent agreement between the asymptotic theory and the direct summation. All these computations were carried out on the AMES CDC 7600 computer, and the results stored on disc. This information has now been transferred to the National Physical Laboratory file store, via magnetic tape, and can be accessed for further processing and graphical display.

5.5 Slow Spatial Growth

The necessary modification of the zero order term of the asymptotic expansion to account fully for slow spatial growth of the boundary layer can be found by an iterative method, in much the same way as for the simple periodic wavetrain. In that case the scaling factor $A(x,\omega)$ could be obtained in terms of integration involving ϕ and its adjoint. Here it turns out that the scaling function A is only a function of ω^*, and again this can be found in terms of ϕ. So far this has not been accomplished, but there does not appear to be any reason why this phase of the problem should not follow through, and values of the coefficients of the ordinary differential equation for $A(\omega^*)$ obtained. This work is planned for the near future.

5.6 Weak Nonlinearity

The further modification (necessarily assumed to be weak), to take account of the nonlinear terms in the equations of motion should also be amenable to an iterative procedure, but so far no attempt has been made in this direction.

6. Summary

Turbulent spots evolving in a laminar boundary layer on a nominally zero pressure gradient flat plate were visualized using novel visualization techniques that utilize fluorescent dye and laser. The extra degree of freedom provided by using fluorescent dye was found to be quite effective in revealing the structure of a turbulent spot. The spot appeared to be composed of a random collection of turbulent eddies which seemed independent of each other, much as in a turbulent boundary layer. Away from the wall, the spot grew by adding more eddies to this collection. The visualization results indicated that at the higher elevations, the eddies were preferentially added to the rear of the spot while always maintaining an arrowhead shape. The entrainment of nonturbulent fluid in planes normal to the wall involved the large scale eddies in a gulping process similar to a fully developed turbulent boundary layer.

Close to the wall, the spanwise growth of the spot seemed to involve another mechanism in addition to that of classical entrainment. The growth in this direction was an order of magnitude greater than that normal to the wall. The present visualization results show that the turbulent diffusion is much less than the growth of the spot boundary in the lateral direction, contrary to the classical ideas of entrainment. Hence, some additional means of turbulent generation must be present.

The augmented growth in the spanwise direction may be due to a destabilization process, as suggested by Corrsin & Kistler (1955). We term this process *"growth by destabilization."* The turbulent eddies within the approaching spot may induce perturbations into the surrounding unstable laminar boundary layer. These fluctuations grow and breakdown forming new turbulence without ever being in contact with the older turbulence. The sequence from which Figure 4 was extracted seemed to indicate a growing, propagating wave-like motion near the wall. Its amplitude was sufficiently large that, directly before being overtaken by the spot, the dye line was displaced approximately 0.2 δ_ℓ . It was impossible to ascertain whether the wave-like structure broke down and formed the new turbulence on the leading edge of the spot, or whether the existing turbulence overran the wave. Further experiments are being pursued to elucidate this process.

The turbulent spots were modulated using two external effects. In the first, spots were generated in a dilute polymer solution. 50 ppm Polyex, WSR-301 solution was prepared before towing the plate. Near the wall, the polymer tended to suppress the small-scale turbulent structures in the spot. Also the lateral growth rate was reduced by about 15 percent, resulting in a more elongated spot. The experiments confirm that the polymer effects are closely associated with wall phenomena. For while the addition of polymer seems to modulate the growth by destabilization mechanism, it does not seem to affect the entrainment mechanism.

The second effect used to modulate a turbulent spot was stratification. Linear, stable density profiles were generated in the towing tank using salt. Brunt-Vaisala frequency in the range 0-0.7 Hz was studied. The stratification inhibits the vertical growth of the turbulent spot. The effect is more pronounced as the density gradient, and hence the Brunt-Vaisala frequency, is increased. The head of the spot collapsed after about 1/4 Brunt-Vaisala period, much the same as a wake collapse in a stratified fluid.

More work is still required to determine the effects of stratification and drag reducing polymers on a turbulent spot. Techniques for improving the visualization in the presence of index of refraction fluctuations are needed to obtain quantitative information on the effects of heavy stratification. The study of spots developing under a wide variety of conditions (e.g. strain-rates) may provide useful insight into the lateral growth mechanism. For example, the wall strain rate in the present experiment was not high enough for polymer induced fluctuations to appear. The effects of those fluctuations on the growth by destabilization mechanism is of great interest to the understanding of that mechanism.

The results of the present visualization study will be greatly enhanced by a series of velocity measurements using a fast response probe, such as laser droppler velocimeter.

The development of a wave packet in a growing boundary layer was investigated analytically. A series representation of the wave packet was discussed. The zero order term in this series is provided by the quasi-parallel flow form of solution defined locally by the Orr-Sommerfield equation. Such a solution can be modified by a weak amplitude scaling factor and the addition of further terms through an iteration procedure. Here the zero order integral has been evaluated by the method of steepest descent and the results compared with numerical summations of the integral. The next stage in the process is to compute this scaling factor and to then see how to extend the calculations to cater for weakly nonlinear effects.

It is hoped that the present research will further our understanding of turbulence and transition. The *"growth by destabilization"* mechanism has been shown to be quite different from classical entrainment. This mechanism does not involve mixing or diffusion, a property that has been always associated with turbulence. This might have important practical consequences.

References

Berman, N. S. and George, W. K. (1974) "Onset of Drag Reduction in Dilute Polymer Solutions," Phys. Fluids 17, 250.

Bertshy, J. R. and Abernathy, F. H. (1977) "Modifications to Laminar and Turbulent Boundary Layers Due to the Addition of Dilute Polymer Solutions," Proc. of the Second Intern. Conf. on Drag Reduction, Cambridge, England.

Blackwelder, R. F. and Kovasznay, L. S. G. (1972) "Time Scales and Correlations in a Turbulent Boundary Layer," Phys. Fluids 15, 1545.

Bouthier, M. (1972) "Stabilite' Linéaire des 'ecoulements Presque Paralléles," J. Mecanique 11, 599.

Burgers, J. M. (1924) "The Motion of a Fluid in the Boundary Layer Along a Plane Smooth Surface," Proc. of the First Intern. Congress of Applied Mech., Delft, 113.

Cantwell, B., Coles, D. and Dimotakis, P. (1978) "Structure and Entrainment in the Plane of Symmetry of a Turbulent Spot," J. Fluid Mech. 87, 641.

Charters, A. C. (1943) "Transition between Laminar and Turbulent Flow by Transverse Contamination," NACA Tech. Note No. 891.

Chen, C-H.P. and Blackwelder, R. (1978) "Large-Scale Motion in a Turbulent Boundary Layer: A Study Using Temperature Contamination," J. Fluid Mech. 89, 1.

Coles, D. and Barker, S. J. (1975) "Some Remarks on a Synthetic Turbulent Boundary Layer," in Turbulent Mixing in Nonreactive and Reactive Flows, ed. S. N. B. Murthy, Plenum, 285.

Corrsin, S. and Kistler, A. L. (1955) "Free-Stream Boundaries of Turbulent Flows," NACA Report No. 1244 (Supersedes NACA TN 3133).

Dhawan, S. and Narasimha, R. (1958) "Some Properties of Boundary Layer Flow During the Transition from Laminar to Turbulent Motion," J. Fluid Mech. 3, 418.

Dryden, H. L. (1934) "Boundary Layer Flow Near Flat Plates," Proc. Fourth Intern. Congress of Applied Mech., Cambridge, England, 175.

Dryden, H. L. (1936) "Airflow in the Boundary Layer Near a Plate," NACA Report No. 562.

Dryden, H. L. (1939) "Turbulence and the Boundary Layer," JAS 6, 85 and 101.

Elder, J. W. (1960) "An Experimental Investigation of Turbulent Spots and Breakdown to Turbulence," J. Fluid Mech. 9, 235.

References (Cont.)

Emmons, H. W. (1951) "The Laminar-Turbulent Transition in a Boundary Layer," J. Aero. Sci. 18, 490.

Falco, R. E (1977) "Coherent Motions in the Outer Region of Turbulent Boundary Layer," Phys. Fluids 20, S124.

Fiedler, H. E. and Head, M. R. (1966) "Intermittency Measurements in a Turbulent Boundary Layer," J. Fluid Mech. 25, 719.

Gaster, M. (1974) "On the Effects of Boundary-Layer Growth on Flow Stability," J. Fluid Mech. 66, 465.

Gaster, M. (1978a) "The Physical Processes Causing Breakdown to Turbulence," 12th Naval Hydrodynamics Symposium, Washington, D. C., 22.

Gaster, M. (1978b) "Series Representation of the Eigenvalues of the Orr-Sommerfeld Equation," J. Comput. Physics 29, 147.

Gaster, M. (1979) "The Propagation of Wave Packets in Laminar Boundary Layers: Asymptotic Theory for Non-Conservative Wave Systems," AIAA Paper 79-1492, 12th Fluid & Plasma Dynamics Conference, Williamsburg, Virginia.

Gaster, M. and Grant, I. (1975) "An Experimental Investigation of the Formation and Development of a Wave Packet in a Laminar Boundary Layer," Proc. R. Soc. Lond. A. 347, 253.

Hama, F. R., Long, J. D., and Hagarety, J. C. (1957) "On Transition from Laminar to Turbulent Flow," J. Appl. Phys. 28, 388.

Klebanoff, P. S. and Tidstrom, K. D. (1959) "Evolution of Amplified Waves Leading to Transition in a Boundary Layer with Zero Pressure Gradient," NASA Tech. Note No. D195.

Klebanoff, P. S., Tidstrom, K. D., and Sargent, L. M. (1962) "The Three-Dimensional Nature of Boundary Layer Instability," J. Fluid Mech. 12, 1.

Kovasznay, L. S. G., Komoda, H., and Vasudeva, B. R. (1962) "Detailed Flow Field in Transition," Proc. Heat Transfer and Fluid Mech. Inst., Standford Univ. Press, 1.

Lin, J.-T. and Pao, Y.-H. (1979) "Wakes in Stratified Fluids," Ann. Review of Fluid Mech. 11, 317.

Mitchener, M. (1954) "Propagation of Turbulence from an Instantaneous Point Disturbance," J. Aero. Sci. 21, 350.

Morkovin, M. V. (1969) "Critical Evaluation of Transition from Laminar to Turbulent Shear Layers with Emphasis on Hypersonically Travelling Bodies," Flight Dyn. Lab. Report No. AFFDL-TR-68-149.

References (Cont.)

Offen, G. R. and Kline, S. J. (1974) "Combined Dye-Streak and Hydrogen-Bubble Visual Observations of a Turbulent Boundary Layer," J. Fluid Mech. 62, 223.

Schlichting, H. (1935) "Amplitudenverteilung und Energiebilanz der kleinen Störungen bei der Plattenströmung," Nachr. Ges. Wiss. Göttingen, Math. Phys. Klasse 1, 47.

Schubauer, G. B. and Skramstad, H. K. (1948) "Laminar Boundary Layer Oscillations on a Flat Plate," NACA Report No. 909.

Schubauer, G. B. and Klebanoff, P. S. (1956) "Contributions on the Mechanics of Boundary Layer Transition," NACA Report No. 1289.

Tani, I. and Hama, F. R. (1953) "Some Experiments on the Effect of a Single Roughness Element on Boundary-Layer Transition," J. Aero. Sci. 20, 289.

Townsend, A. A. (1976) "The Structure of Turbulent Shear Flow," Cambridge Univ. Press.

van der Hegge Zijnen, B. G. (1924) "Measurements of the Velocity Distribution in the Boundary Layer Along a Plane Surface," Thesis, Delft.

Wygnanski, I., Haritonidis, J. H. and Kaplan, R. E. (1979) "On a Tollmien-Schlichting Wave Packet Produced by a Turbulent Spot," J. Fluid Mech. 92, 505.

Wygnanski, I., Sokolove, M., and Friedman, D. (1976) "On a Turbulent 'Spot' in a Laminar Boundary Layer," J. Fluid Mech. 78, 785.

Zilberman, M., Wygnanski, I., and Kaplan, R. (1977) "Transitional Boundary Layer Spot in a Fully Turbulent Environment," Phys. Fluids 20, S258.

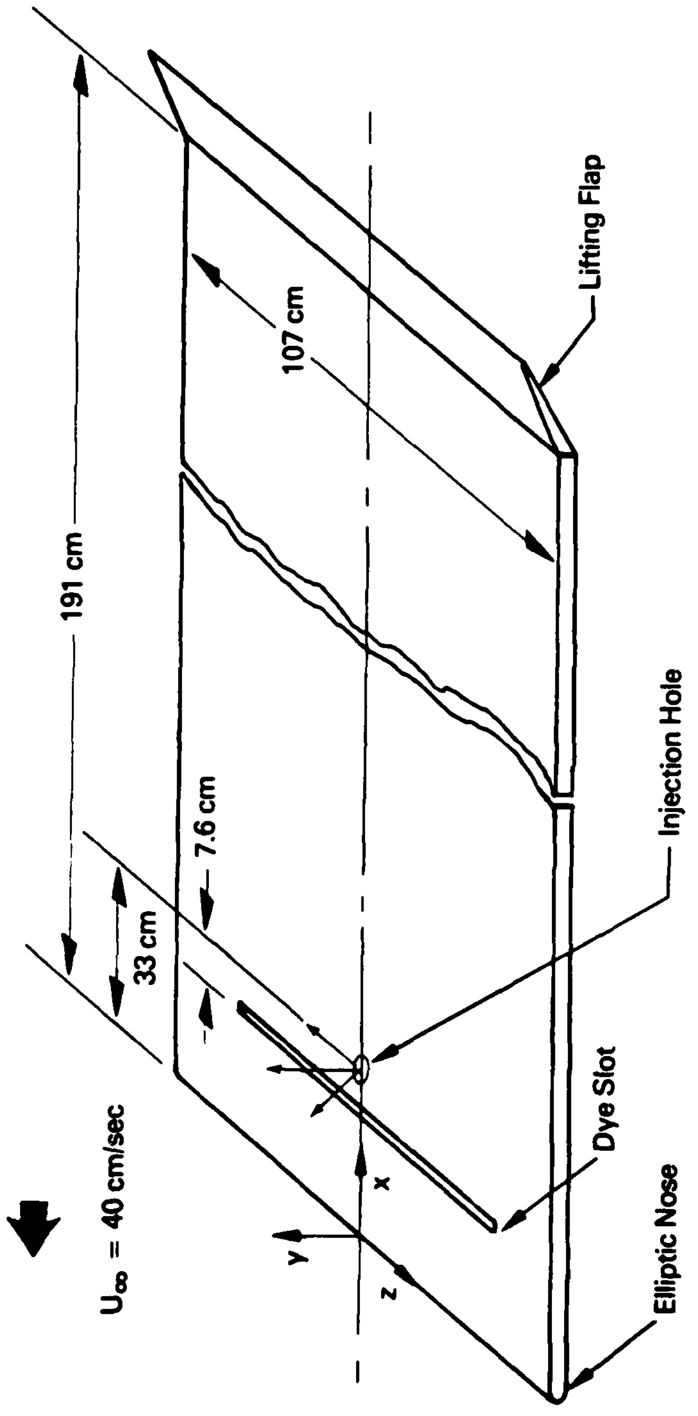

Figure 1. Schematic of the Flat Plate and Coordinate System.

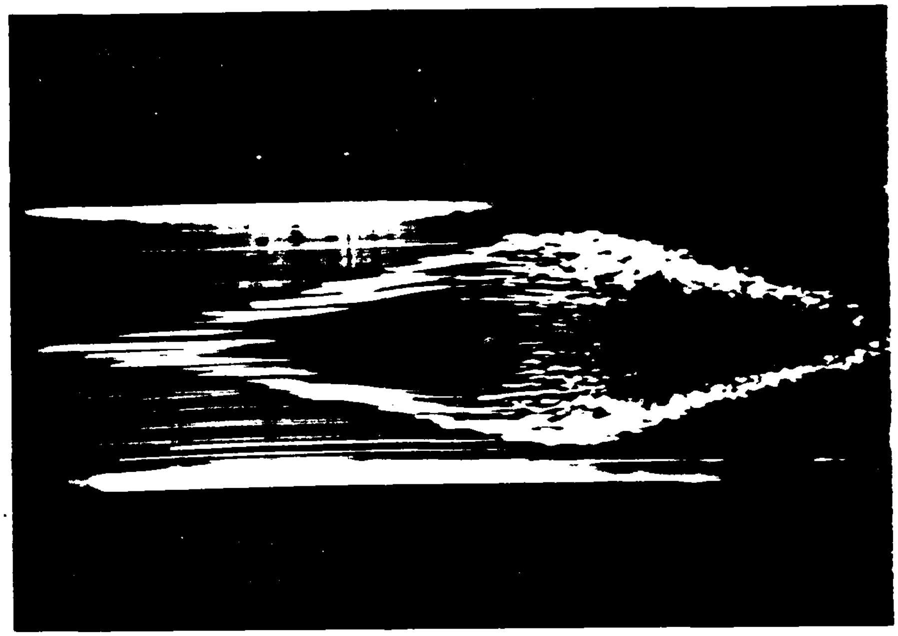

Figure 2. A Plan View of the Turbulent Spot at $y = 0$.

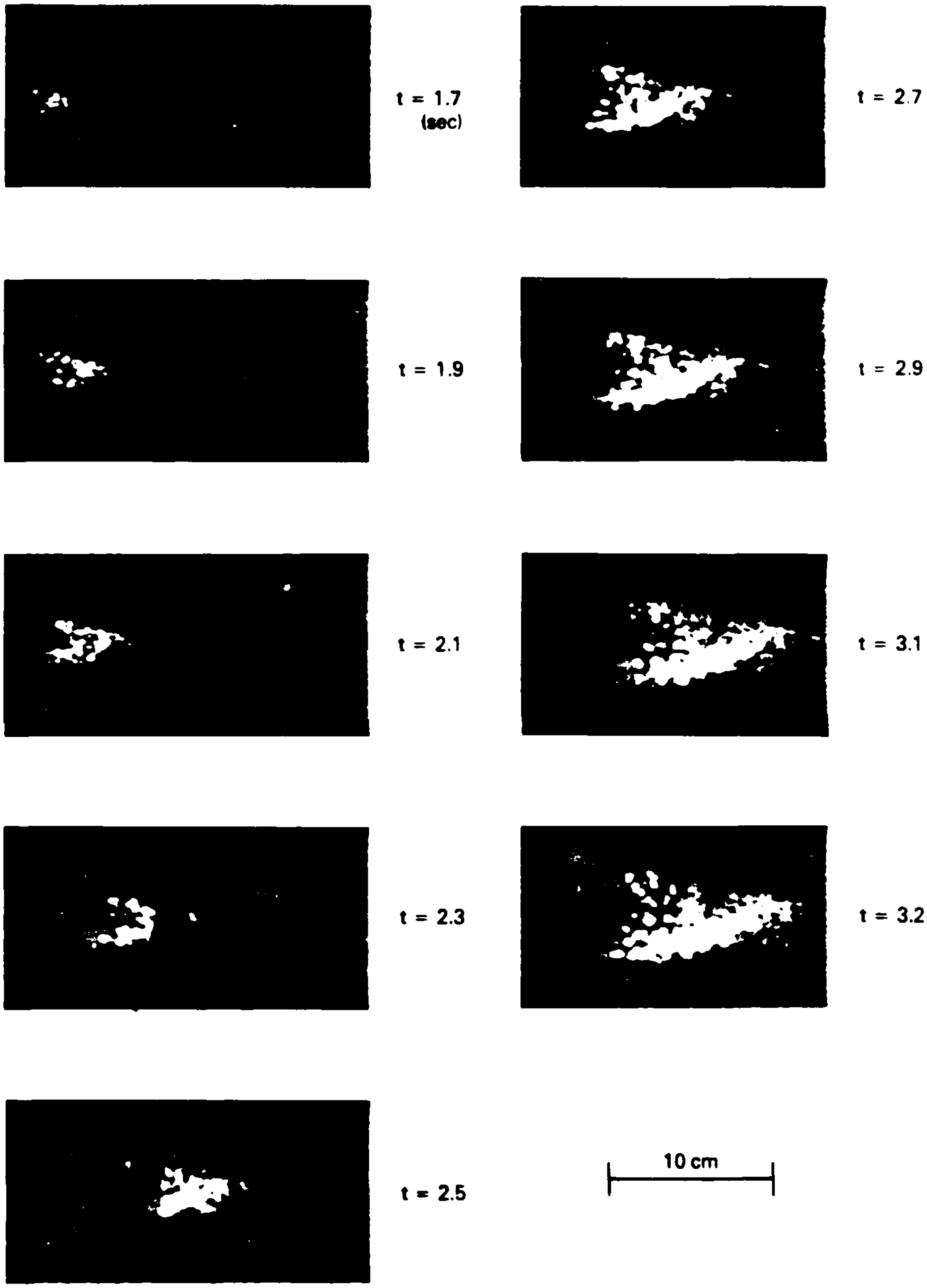

Figure 3. Sequence of Plan Views at y = 1.3 cm, Illustrating the Growth of the Spot. The Time Since the Spot Generation is Indicated to the Right.

Figure 4. Plan View of the Spot at $y = 0.1$ cm. The Dye Line Fixed in the Fluid Undergoes a Large Amplitude Oscillation Before Being Overtaken by the Spot.

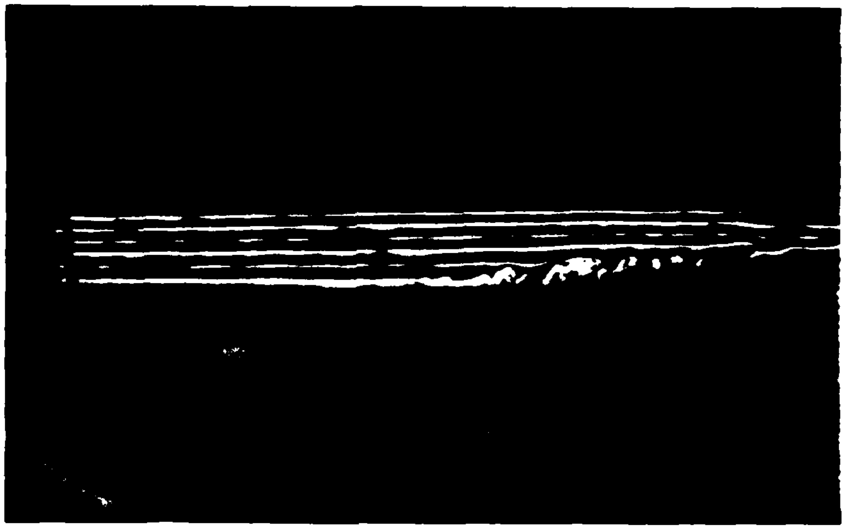

a. z = 0.

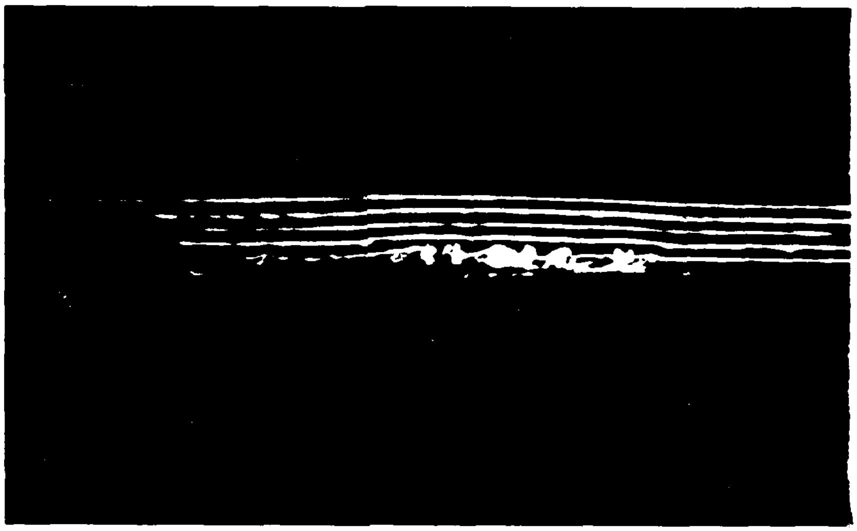

b. z = 6 cm.

Figure 5. Cross-Sectional View in the x-y Plane of the Turbulent Spot at Two Different Spanwise Locations.

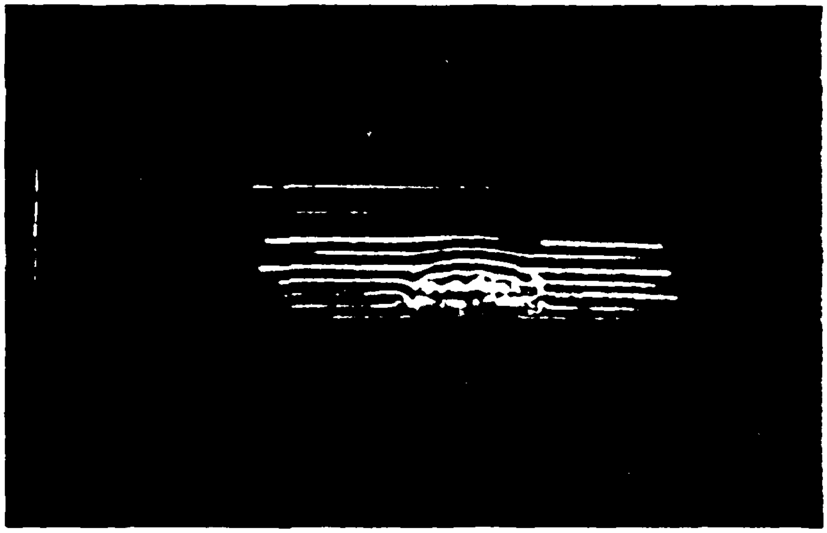

Figure 6. Spanwise Section of the Spot in the y-z Plane.

a. Dye Emanates from the Cylinder Only.

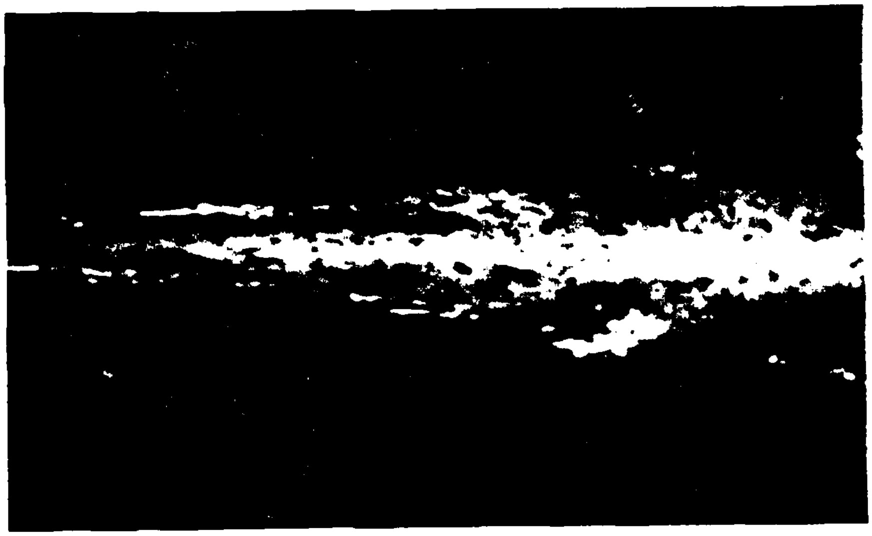

b. Dye is also Allowed to Seep from the Spanwise Slot.

Figure 7. Effects of a Roughness Element in an Unstable Laminar Boundary Layer. The Cylinder is Located at $Rx = 9 \times 10^4$.

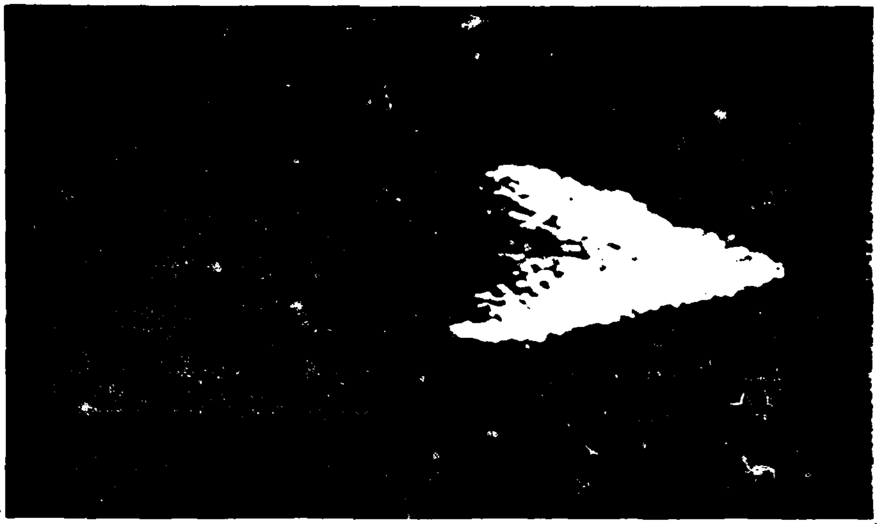

a. Pure Water.

b. 50 ppm WSR-301 Solution.

Figure 8. Plan View of a Turbulent Spot. Sheet of Light is at $y = 3$ mm, and Plate is Towed at 40 cm/sec.

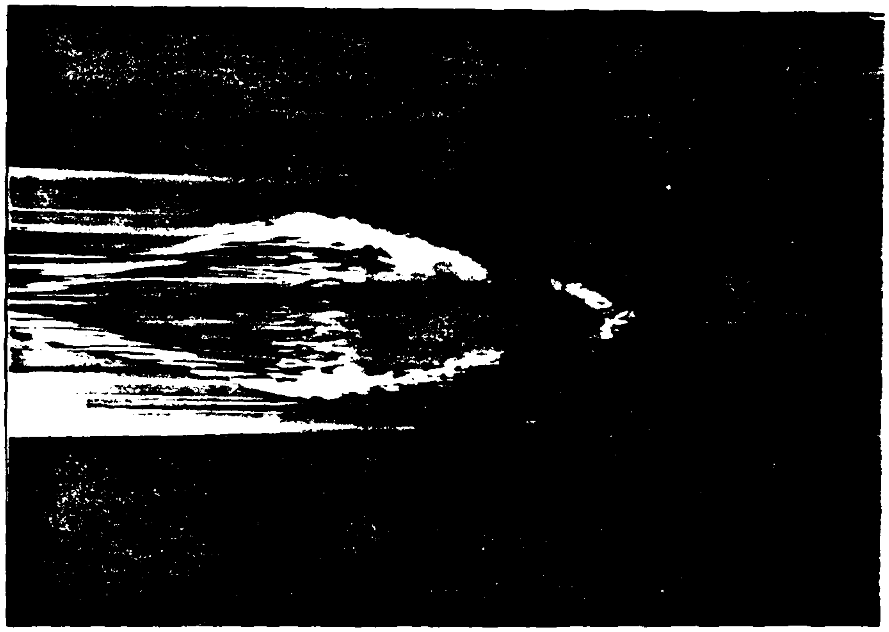

Figure 9. Plan View of a Turbulent Spot in 50 ppm WSR-301 Solution. Sheet of Light at $y = 0$, and Plate is Towed at 60 cm/sec.

a. Pure Water.

b. 50 ppm WSR-301 Solution.

Figure 10. Cross-Sectional View in the x-y Plane of a Turbulent Spot. Sheet of Light at z = 6 cm, and Plate is Towed at 40 cm/sec.

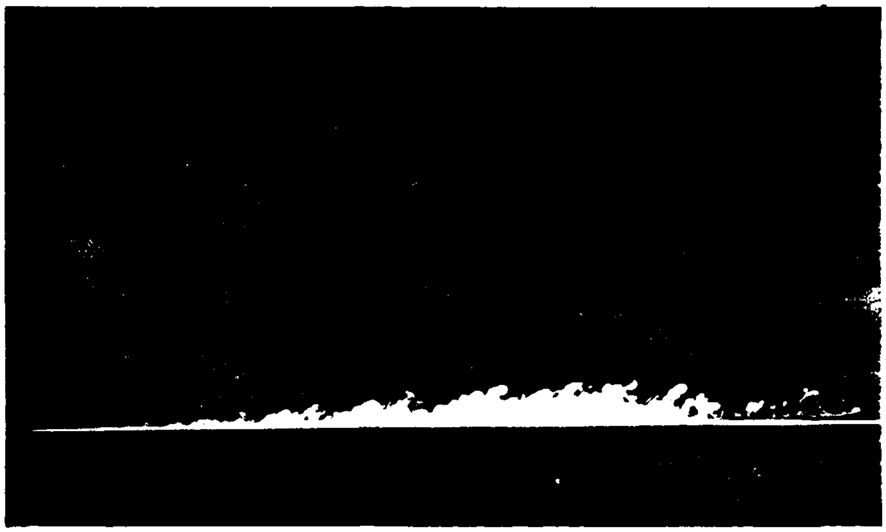

a. Homogeneous Fluid.

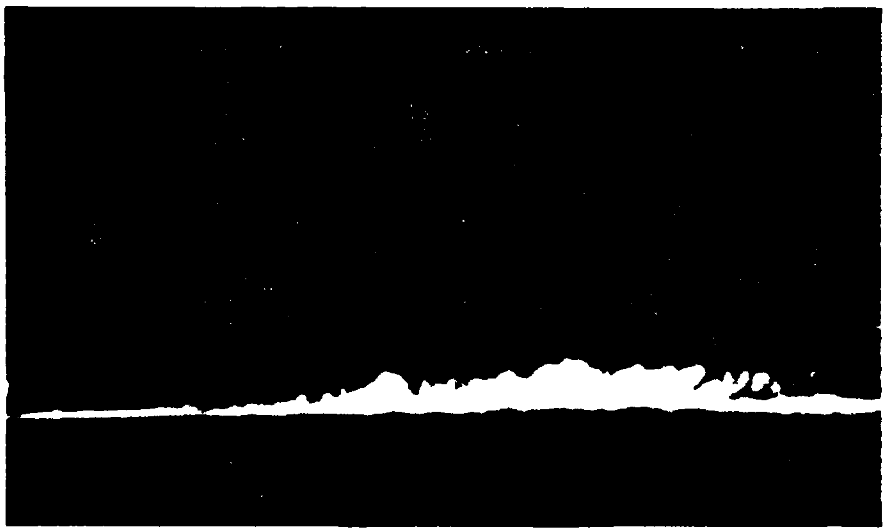

b. Stratified Fluid; $N = 0.1$ Hz.

Figure 11. Cross-Sectional View in the x-y Plane. Sheet of Light at $z = 0$ cm, and Plate is Towed at 40 cm/sec.

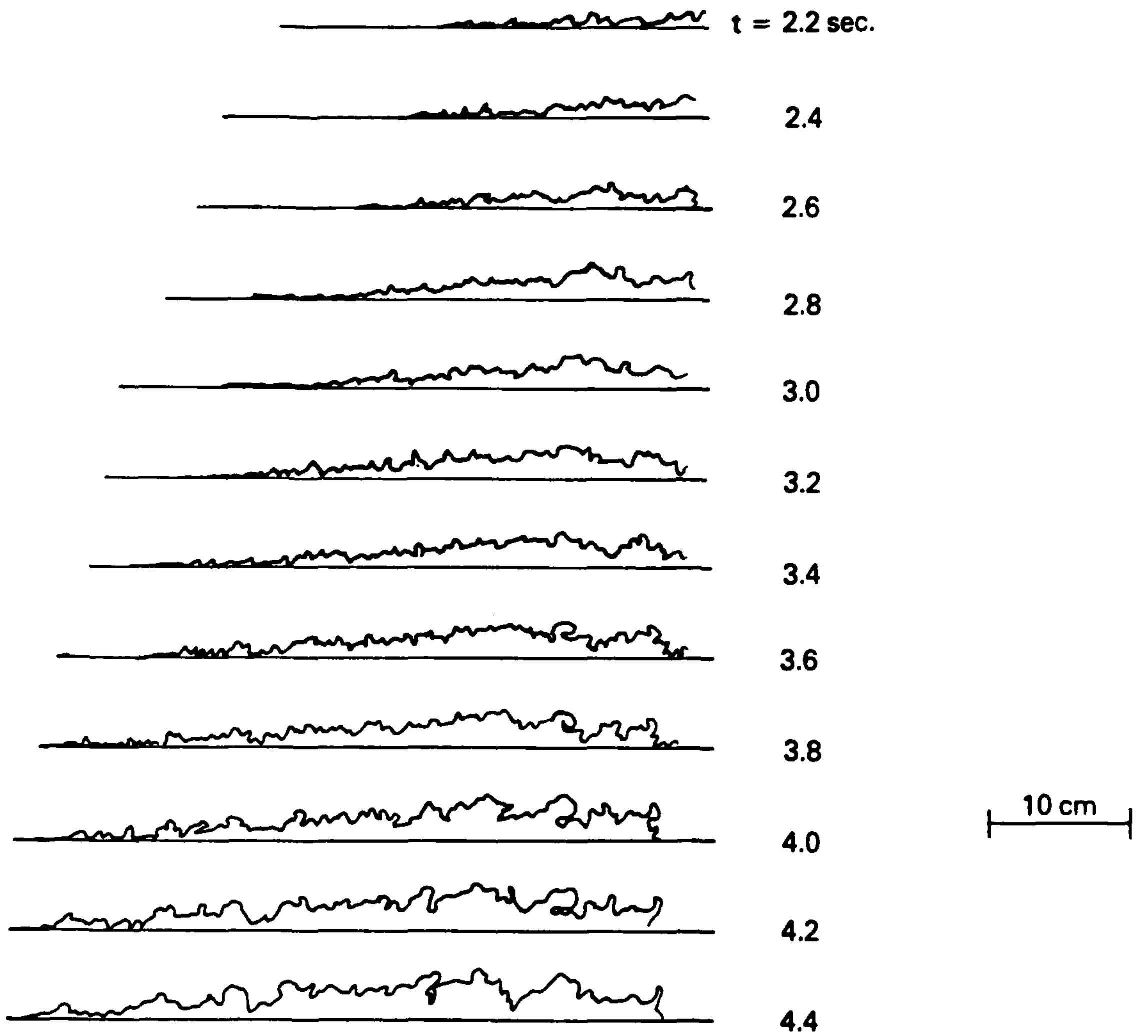

a. Homogeneous Fluid.

Figure 12. Traces From Movie Frames Showing Cross-Sectional View of an Evolving Turbulent Spot; $z = 0$, $U_{\infty} = 40$ cm/sec.

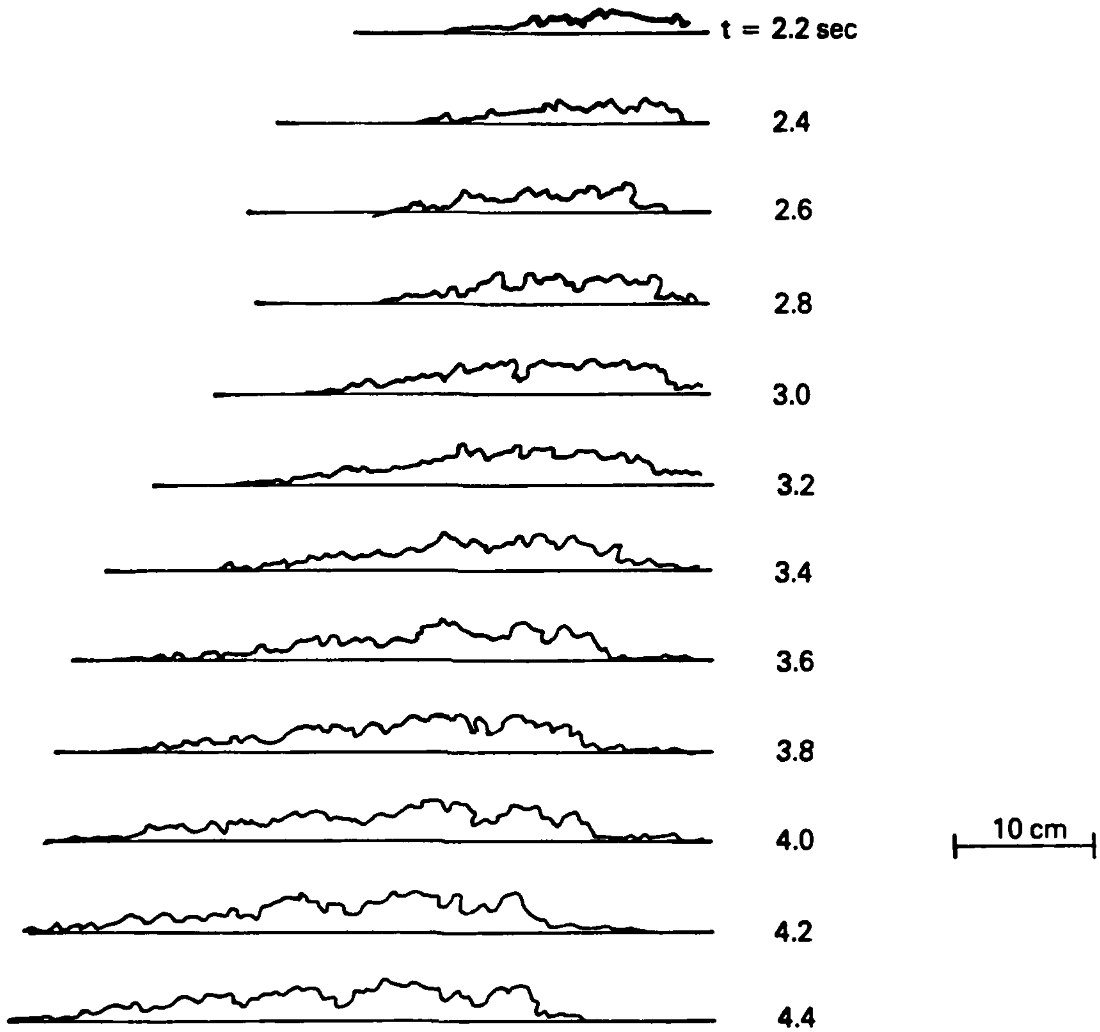

b. Stratified Fluid; N = 0.1 Hz.

Figure 12. Traces From Movie Frames Showing Cross-Sectional View of an Evolving Turbulent Spot; z = 0, U_∞ = 40 cm/sec. (Cont.).

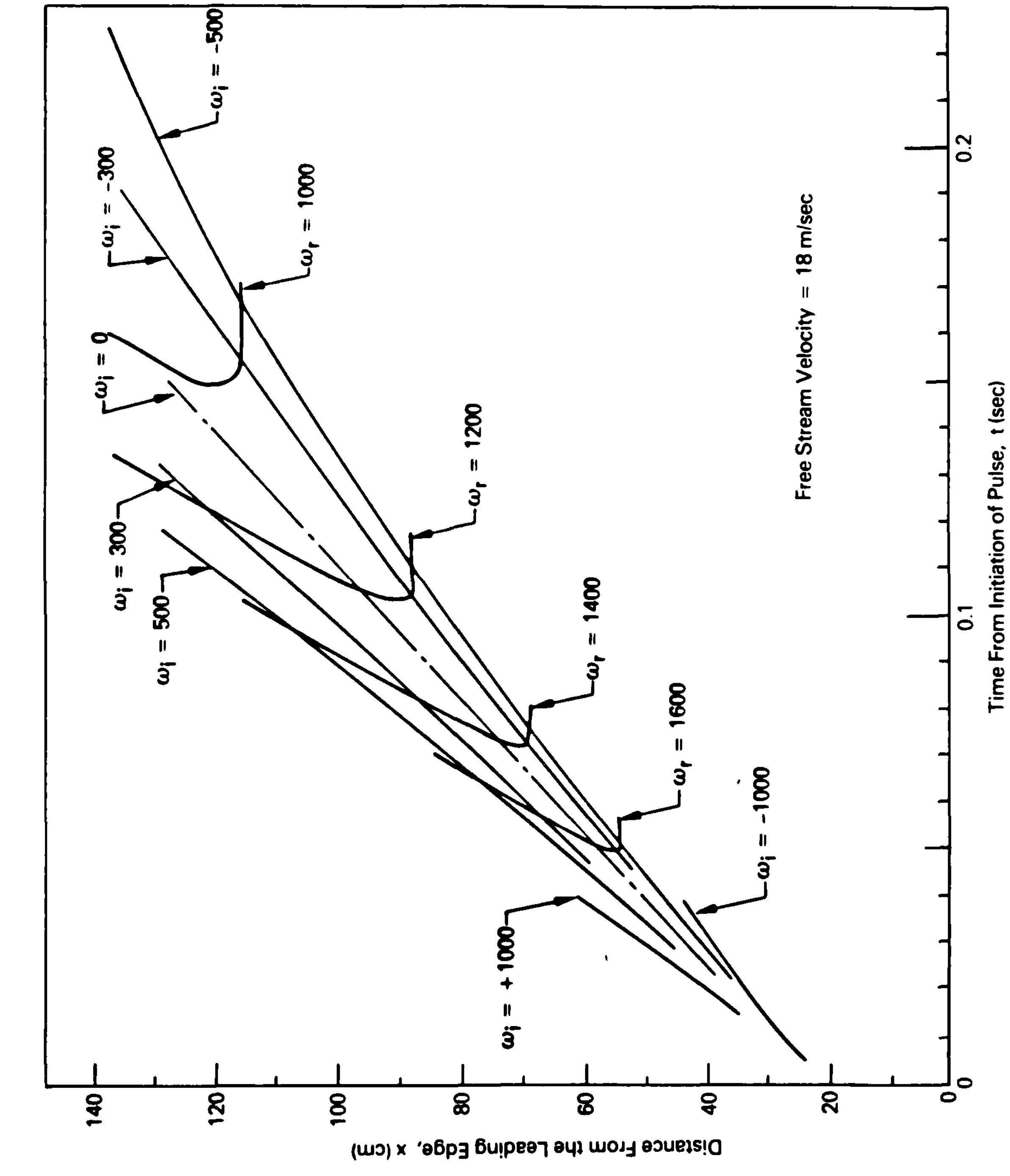

Figure 13. Values of ω^* Given by Equation (8).